Supporting Information for:

Uncovering the Roles of Oxygen in Cr(III) Photoredox Catalysis

Robert F. Higgins,[†] Steven M. Fatur,[‡] Samuel G. Shepard,[‡] Susan M. Stevenson,[§] David J. Boston,[†] Eric M. Ferreira,[§] Niels H. Damrauer,[‡] Anthony K. Rappé,[†,*] Matthew P. Shores[†,*]

[†] Department of Chemistry, Colorado State University, Fort Collins, Colorado 80523-1872, USA
[§] Department of Chemistry, University of Georgia, Athens, Georgia 30602, USA
[‡] Department of Chemistry and Biochemistry, University of Colorado, Boulder, Colorado 80309-0215, USA

Table of Contents:

Catalysis Studies

Standard cycloaddition procedure

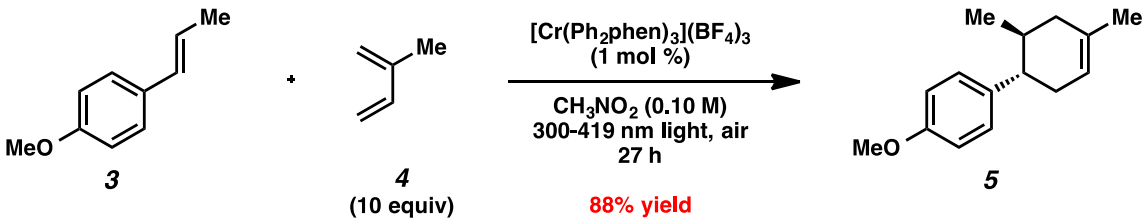

Cyclohexene 5. To a flame-dried 2-dram borosilicate vial open to air was added *para*-anethole (**3**) (17.7 mg, 0.120 mmol), isoprene (**4**) (0.120 mL, 1.20 mmol), $[Cr(Ph_2phen)_3](BF_4)_3$ (1.6 mg, 0.00120 mmol), and nitromethane (1.20 mL). The vial was capped and placed in a Rayonet photochemical reactor equipped with 419, 350, and 300 nm light bulbs. The reaction was irradiated with stirring until consumption of *para*-anethole (**3**) was complete, as determined by TLC (27 h). The reaction was then diluted with H_2O (1.5 mL) and transferred to a separatory funnel. The layers were separated and the aqueous layer was extracted with Et_2O (3 × 2 mL). The combined organic layers were washed with brine (8 mL), and dried over Na_2SO_4. The volatile materials were removed by rotary evaporation, and the resulting residue was purified by flash chromatography (100% hexanes → 9:1 hexanes/EtOAc eluent) to afford cycloadduct **5** (22.7 mg, 88% yield) as a colorless oil.

All spectroscopic data were consistent with previously reported values.[1]

Degassed cycloaddition experiments

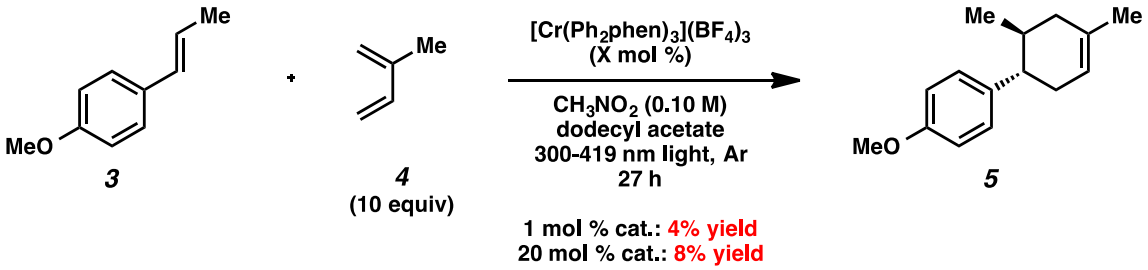

1 mol % catalyst: To a 25-mL Schlenk flask was added *para*-anethole (**3**) (14.8 mg, 0.100 mmol), isoprene (**4**) (0.100 mL, 1.00 mmol), $[Cr(Ph_2phen)_3](BF_4)_3$ (1.3 mg, 0.00100 mmol), nitromethane (1.00 mL), and dodecyl acetate (22.8 mg, 0.100 mmol) as an internal standard. The flask was sealed, and the reaction mixture was degassed by 3 freeze-pump-thaw cycles and put under Ar. The reaction was then placed in a Luzchem photoreactor equipped with 419, 350, and 300 nm light bulbs. The reaction mixture was irradiated with stirring for 27 h. The reaction mixture was then passed through a short plug of silica (2.5 cm high × 1 cm wide, Et_2O eluent). The volatile materials were removed by rotary evaporation, and the resulting residue was analyzed by ^1H NMR. Based on the integrations of the product alkene peak at 5.44 ppm and the internal standard triplet at 4.05 ppm, product **5** was formed in 4% yield.

20 mol % catalyst: To a 25-mL Schlenk flask was added *para*-anethole (**3**) (7.4 mg, 0.0500 mmol), isoprene (**4**) (0.0500 mL, 0.500 mmol), $[Cr(Ph_2phen)_3](BF_4)_3$ (13.1 mg, 0.0100 mmol), nitromethane (0.500 mL), and dodecyl acetate (11.4 mg, 0.0500 mmol) as an internal standard. The flask was sealed, and the reaction mixture was degassed by 3 freeze-pump-thaw cycles and put under Ar. The reaction was then placed in a Luzchem photoreactor equipped with 419, 350, and 300 nm light bulbs. The reaction mixture was irradiated with stirring for 27 h. The reaction mixture was then passed through a short plug of silica (2.5 cm high × 1 cm wide, Et_2O eluent). The volatile materials were removed by rotary evaporation, and the resulting residue was analyzed by ^1H NMR. Based on the integrations of the product alkene peak at 5.44 ppm and the internal standard triplet at 4.05 ppm, product **5** was formed in 8% yield.

Cycloadditions with additives

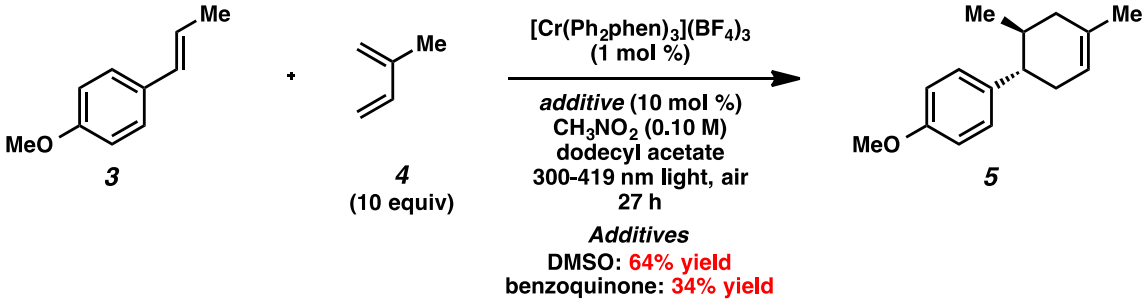

To a 2-dr vial open to air was added *para*-anethole (**3**) (14.8 mg, 0.100 mmol), isoprene (**4**) (0.100 mL, 1.00 mmol), $[Cr(Ph_2phen)_3](BF_4)_3$ (1.3 mg, 0.00100 mmol), nitromethane (1.00 mL), additive (see below), and dodecyl acetate (22.8 mg, 0.100 mmol) as an internal standard. The vial was capped, and the reaction mixture was placed in a Luzchem photoreactor equipped with 419, 350, and 300 nm light bulbs. The reaction mixture was irradiated with stirring for 27 h. The reaction mixture was then passed through a short plug of silica (2.5 cm high × 1 cm wide, Et_2O eluent). The volatile materials were

removed by rotary evaporation, and the resulting residue was analyzed by ^{1}H NMR. Yields were determined by comparing the integrations of the product alkene peak at 5.44 ppm and the internal standard triplet at 4.05 ppm.

Additive amount and yield of cyclohexene **5**:

- DMSO (0.7 µL, 0.0100 mmol); 64% yield
- benzoquinone (1.1 mg, 0.0100 mmol); 34% yield

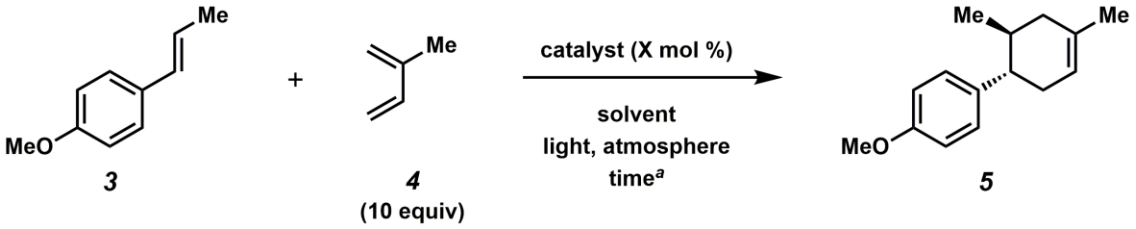

Solvent	Atmosphere	Yield (%) $[Cr(Ph_2phen)_3](BF_4)_3$ (1 mol %)	$[Ru(bpz)_3](PF_6)_2$ (1 mol %)	$[Ru(bpz)_3](BArF)_2$ (0.5 mol %)[b]
CH_3NO_2	air	88	87[c]	
CH_3NO_2	degas, Ar	4[c]	88[c]	
CH_2Cl_2	air	50	0[d]	98
CH_2Cl_2	degas, Ar	12[c]	0[d]	46
CH_3NO_2 (+ 25 mol % benzoquinone)	air	2		
CH_3NO_2 (+ 50 mol % benzoquinone)	air	2		
CH_3NO_2 (+ 1 mol % KO_2)	air	2		
CH_2Cl_2 (+ 1 mol % KO_2)	air	0		
CH_2Cl_2 (+ 1 equiv KO_2)	degas, Ar	0		

[a] Cr reactions were run for 27 h; Ru reactions were run for 1 h. [b] Yoon's results, 3 equiv diene. [c] Yields determined by ^{1}H NMR with dodecyl acetate as an internal standard. [d] Catalyst not soluble in CH_2Cl_2; no reaction.

Cycloadditions with 1-substituted dienes

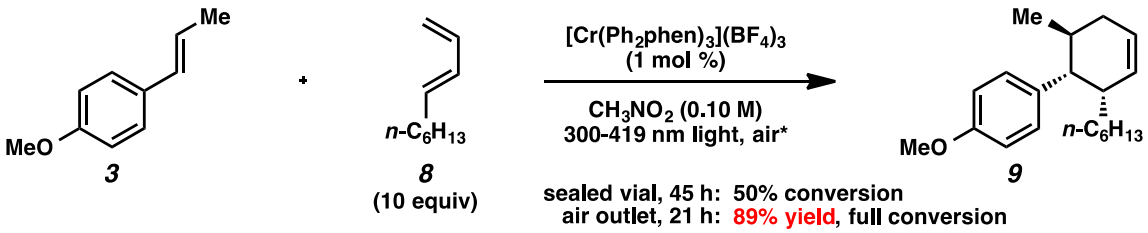

sealed vial, 45 h: 50% conversion
air outlet, 21 h: 89% yield, full conversion

Sealed vial: To a flame-dried 2-dram borosilicate vial open to air was added *para*-anethole (**3**) (7.4 mg, 0.0500 mmol), diene **8** (69.1 mg, 0.500 mmol), $[Cr(Ph_2phen)_3](BF_4)_3$ (0.7 mg, 0.000500 mmol), and nitromethane (0.500 mL). The vial was capped and placed in a Rayonet photochemical reactor equipped with 419, 350, and 300 nm light bulbs. The reaction was irradiated with stirring for 45 h. The reaction was then diluted with H_2O (1.5 mL) and transferred to a separatory funnel. The layers were separated and the aqueous layer was extracted with pentane (3 × 2 mL). The combined organic layers were washed with brine (8 mL), and dried over Na_2SO_4. The volatile materials were removed by rotary evaporation, and the resulting residue analyzed by ^1H NMR. Based on the integrations of the aryl peaks of *para*-anethole (**3**) and cycloadduct **9**, ~50% conversion to product **9** was achieved.

Air outlet: To a flame-dried 2-dram borosilicate vial open to air was added *para*-anethole (**3**) (17.7 mg, 0.120 mmol), diene **8** (0.166 g, 1.20 mmol), $[Cr(Ph_2phen)_3](BF_4)_3$ (1.6 mg, 0.00120 mmol), and nitromethane (1.20 mL). The vial was equipped with a septum cap with a needle outlet and placed in a Rayonet photochemical reactor equipped with 419, 350, and 300 nm light bulbs. The reaction was irradiated with stirring until consumption of *para*-anethole (**3**) was complete, as determined by TLC (21 h). The reaction was then diluted with H_2O (1.5 mL) and transferred to a separatory funnel. The layers were separated and the aqueous layer was extracted with pentane (3 × 2 mL). The combined organic layers were washed with brine (8 mL), and dried over Na_2SO_4. The volatile materials were removed by rotary evaporation, and the resulting residue was purified by flash chromatography (100% hexanes → 9:1 hexanes/EtOAc eluent) to afford cycloadduct **9** (30.7 mg, 89% yield) as a colorless oil. All spectroscopic data were consistent with previously reported values.[2]

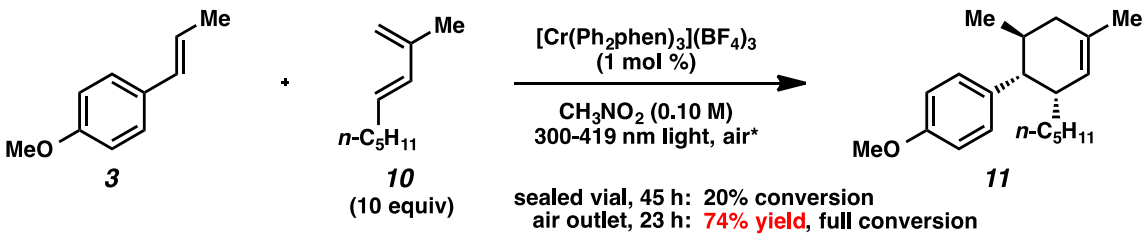

Sealed vial: To a flame-dried 2-dram borosilicate vial open to air was added *para*-anethole (**3**) (7.4 mg, 0.0500 mmol), diene **10** (69.1 mg, 0.500 mmol), $[Cr(Ph_2phen)_3](BF_4)_3$ (0.7 mg, 0.000500 mmol), and nitromethane (0.500 mL). The vial was capped and placed in a Rayonet photochemical reactor equipped with 419, 350, and 300 nm light bulbs. The reaction was irradiated with stirring for 45 h. The reaction was then diluted with H_2O (1.5 mL) and transferred to a separatory funnel. The layers were separated and the aqueous layer was extracted with pentane (3 × 2 mL). The combined organic layers were washed with brine (8 mL), and dried over Na_2SO_4. The volatile materials were removed by rotary evaporation, and the resulting residue analyzed by ^1H NMR. Based on the integrations of the aryl peaks of *para*-anethole (**XX3**) and cycloadduct **11**, ~20% conversion to product **11** was achieved.

Air outlet: To a flame-dried 2-dram borosilicate vial open to air was added *para*-anethole (**3**) (17.7 mg, 0.120 mmol), diene **10** (0.166 g, 1.20 mmol), $[Cr(Ph_2phen)_3](BF_4)_3$ (1.6 mg, 0.00120 mmol), and nitromethane (1.20 mL). The vial was equipped with a septum cap with a needle outlet and placed in a Rayonet photochemical reactor equipped with 419, 350, and 300 nm light bulbs. The reaction was irradiated with stirring until consumption of *para*-anethole (**3**) was complete, as determined by TLC (23 h). The reaction was then diluted with H_2O (1.5 mL) and transferred to a separatory funnel. The layers were separated and the aqueous layer was extracted with pentane (3 × 2 mL). The combined organic

layers were washed with brine (8 mL), and dried over Na_2SO_4. The volatile materials were removed by rotary evaporation, and the resulting residue was purified by flash chromatography (100% hexanes → 9:1 hexanes/EtOAc eluent) to afford cycloadduct **11** (25.4 mg, 74% yield) as a colorless oil. All spectroscopic data were consistent with previously reported values.[2]

Photophysical Experimental

Samples of the photocatalyst dissolved in 3.0 mL nitromethane were prepared in 1 cm × 1 cm quartz cuvettes with an absorbance of ~0.1 at the excitation wavelength, 400 nm. Addition of a known volume of a stock solution of the quencher dissolved in nitromethane was used to achieve the desired concentration. The excitation source was the output of a Ti:Sapphire laser system (Clark MXR CPA1000, NJA-5, ≈800 ± 10 nm, ≈150 fs temporal fwhm, 1 kHz, 500 mJ/pulse) that was then passed through a 100 μm crystal of β-barium borate (Type I, 30°) to generate the second harmonic of the fundamental (centered around 400 nm) and attenuated with neutral density filters to ~10μJ/pulse. A short pass filter was used to remove the residual fundamental. Following excitation with an unfocused 400 nm beam, emission was collected at a right angle and measured through a ~15 nm bandpass filter centered at 750 nm using a Hamamatsu H9305-02 photomultiplier tube (PMT) operating at – 900 Vdc. The PMT response was recorded using a LeCroy 9384L Oscilloscope and averaged over 1000 scans. It was confirmed that the measured signal was linear in the power range of our experiments. The resulting data were fit using Igor Pro 6.37 (WaveMetrics) and a single exponential decay function. Quenching rate constants were obtained from the measured τ values using the Stern-Volmer equation. All experiments were performed at room temperature.

The chemical actinometer of potassium ferrioxalate was used to quantify the photon flux of the light source following the procedures outlined in literature.[3,4] An NMR tube and a 0.5 dram vial were both charged with 0.60 mL of the actinometer solution. The NMR tube is then irradiated with 419 nm light for 30 seconds while the vial is kept in similar conditions without irradiation. Each solution is added to a vial containing 1.5 mL of the 0.1% phenanthroline solution and allowed to sit for 30 minutes in the dark. The UV-vis of the two solutions are taken and the absorbance at 510 nm is recorded.[3] All of the photolysis experiments followed the same general procedure. An NMR tube is charged with 0.80 mg $[Cr(Ph_2phen)_3](BF_4)_3$, 8.83 μL (8.85 mg) trans-anethole, 60 μL (40.86 mg) isoprene, 1 μL (0.86 mg) mestylene and 600 μL of solvent. The reactions were monitored by ^1H NMR, using an internal standard to calculate concentrations of the product.

Electrochemical Data

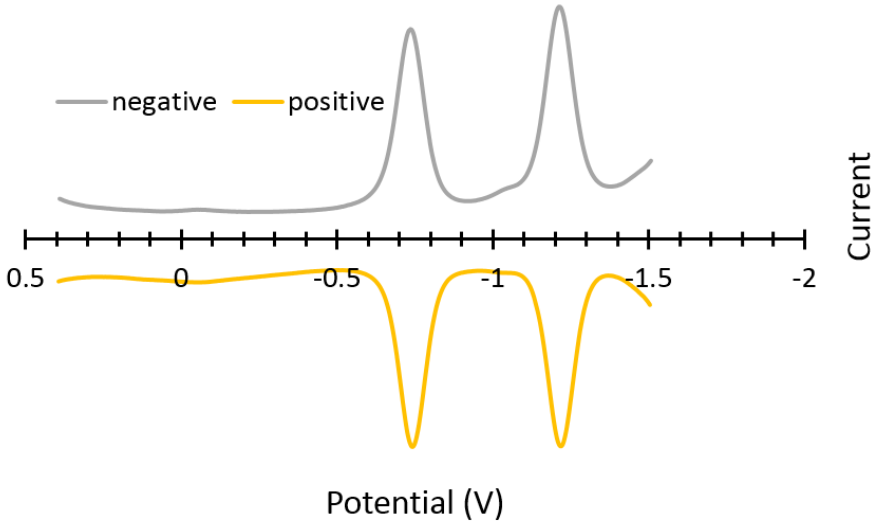

Figure S1. SWVs of **2** in a 0.1 M nitromethane solution of Bu_4NPF_6 referenced to Fc^+/Fc where the designations negative and positive indicate the step-direction. Each voltammogram was begun at either the most anodic or cathodic potential dependent on the scan direction.

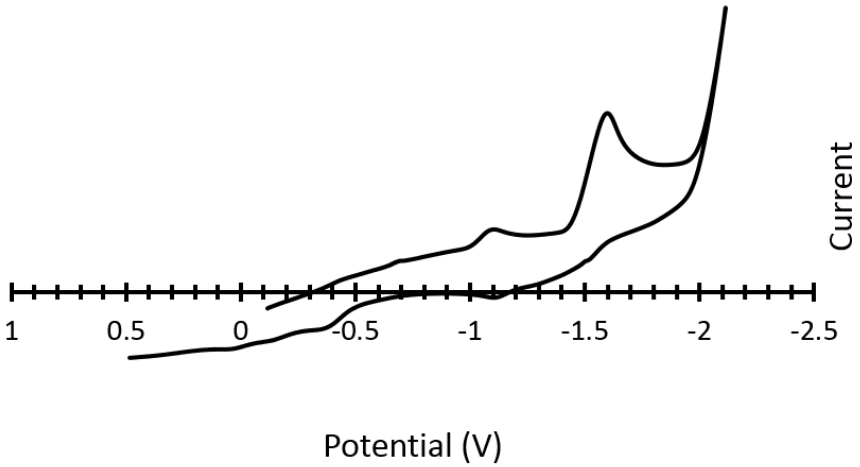

Figure S2. CV of **2** in a 0.1 M nitromethane solution of Bu_4NPF_6 referenced to Fc^+/Fc in darkness with O_2 bubbled through performed at 100 mV/s. The scans were all started at the rest potential of the cell (-0.1154 V) and swept cathodic.

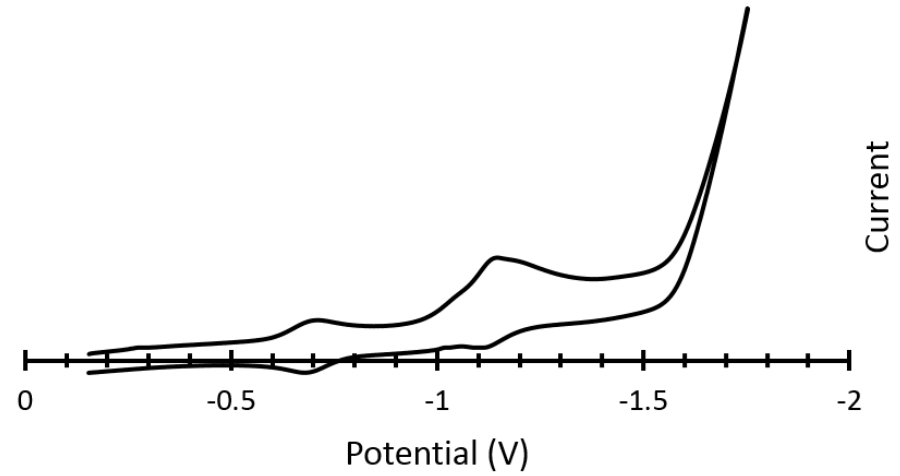

Figure S3. CV of **2** in a 0.1 M nitromethane solution of Bu_4NPF_6 referenced to Fc^+/Fc with isoprene added performed at 100 mV/s. The scans were all started at the rest potential of the cell (-0.1681 V) and swept cathodic.

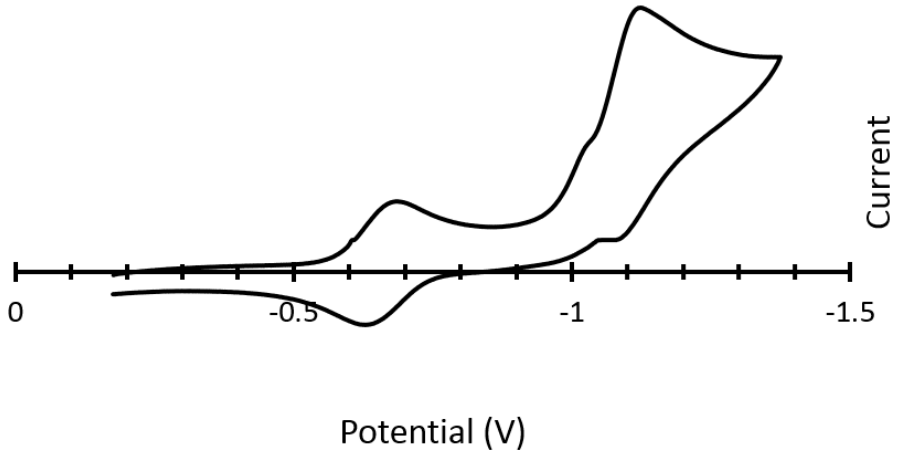

Figure S4. CV of **2** in a 0.1 M nitromethane solution of Bu_4NPF_6 referenced to Fc^+/Fc with anethole added performed at 100 mV/s. The scans were all started at the rest potential of the cell (-0.1867 V) and swept cathodic.

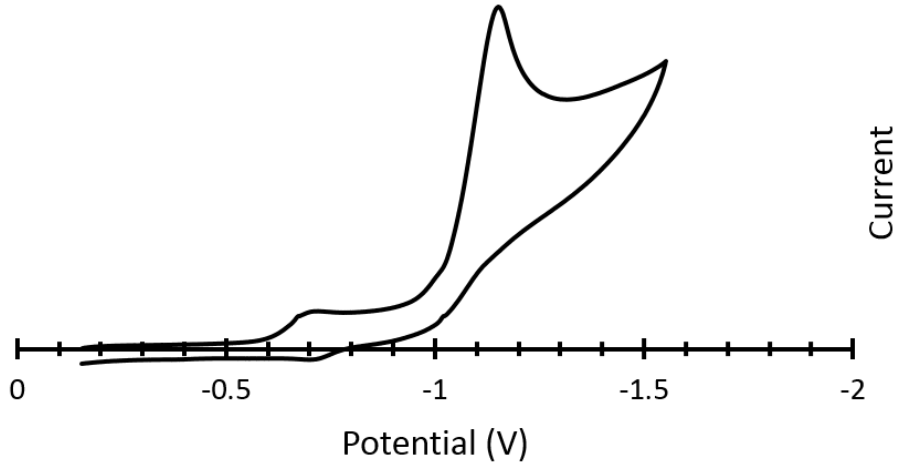

Figure S5. CV of **2** in a 0.1 M nitromethane solution of Bu_4NPF_6 referenced to Fc^+/Fc with anethole and isoprene added with O_2 bubbled through performed at 100 mV/s. The scans were all started at the rest potential of the cell (-0.1666 V) and swept cathodically.

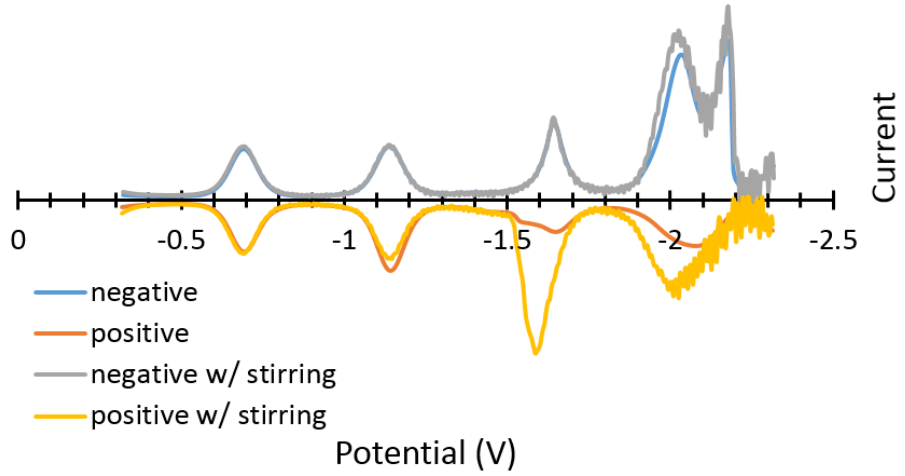

Figure S6. SWVs of **2** in a 0.1 M acetonitrile solution of Bu_4NPF_6 referenced to Fc^+/Fc where the designations negative and positive indicate the step-direction. Each voltammogram was begun at either the most anodic or cathodic potential, depending on the scan direction.

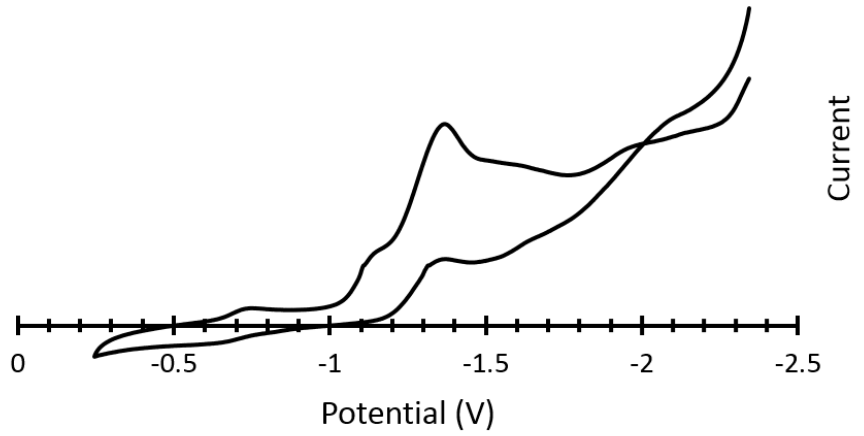

Figure S7. CVs of **2** in a 0.1 M acetonitrile solution of Bu_4NPF_6 referenced to Fc^+/Fc after O_2 was bubbled through. The scans were all started at the rest potential of the cell (-0.4892 V) and swept cathodically.

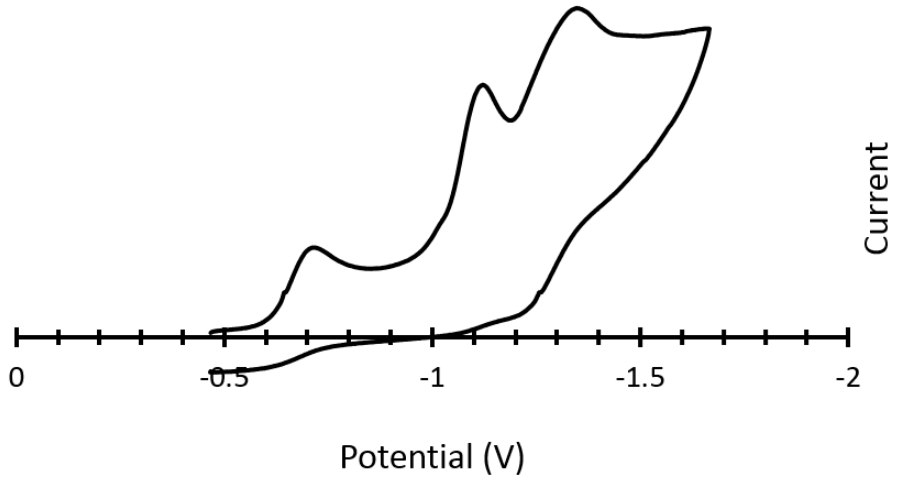

Figure S8. CV of **2** in a 0.1 M acetonitrile solution of Bu_4NPF_6 referenced to Fc^+/Fc after isoprene and anethole were added performed at 100 mV/s. The scans were all started at the rest potential of the cell (-0.4826 V) and swept cathodically.

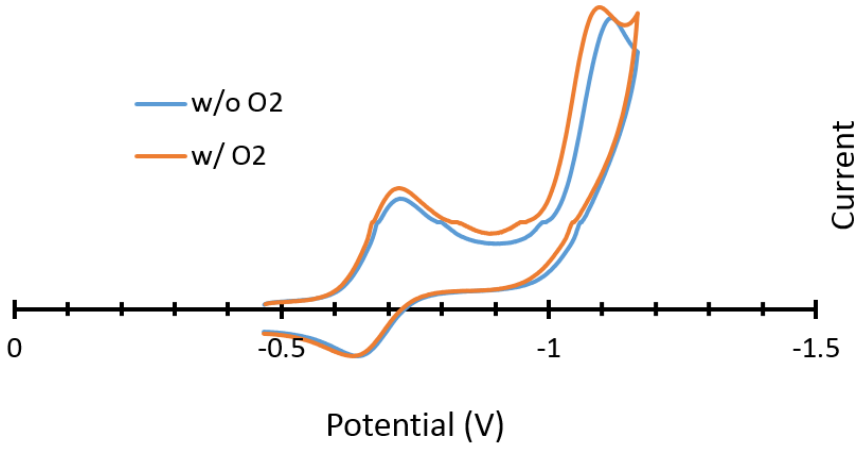

Figure S9. CVs of **2** in a 0.1 M acetonitrile solution of Bu_4NPF_6 referenced to Fc^+/Fc after isoprene and anethole were added performed at 100mV/s. The scans were all started at the rest potential of the cell (-0.4786 V) and swept cathodically.

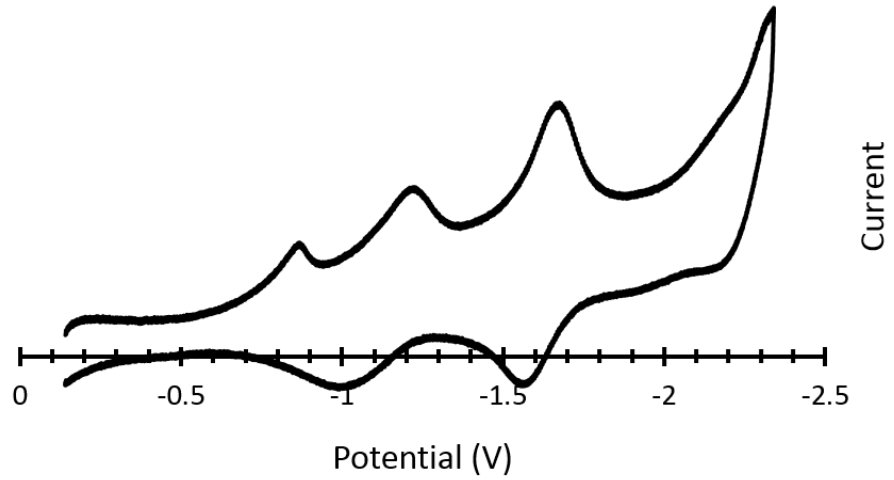

Figure S10. CVs of **2** in a 0.1 M dichloromethane solution of Bu_4NPF_6 referenced to Fc^+/Fc. The scans were all started at the rest potential of the cell (-0.1412 V) and swept cathodically.

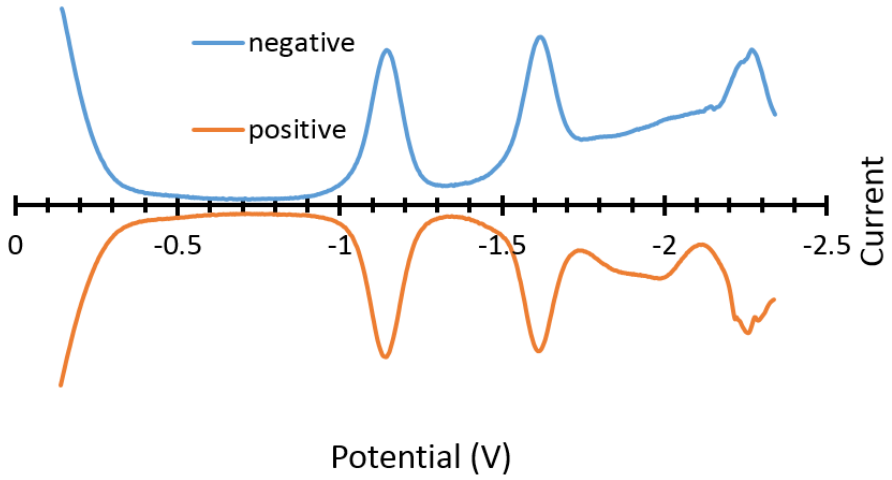

Figure S11. SWVs of **2** in a 0.1 M dichloromethane solution of Bu_4NPF_6 referenced to Fc^+/Fc where the designations negative and positive indicate the step-direction. Each voltammogram was begun at either the most anodic or cathodic potential, depending on the scan direction.

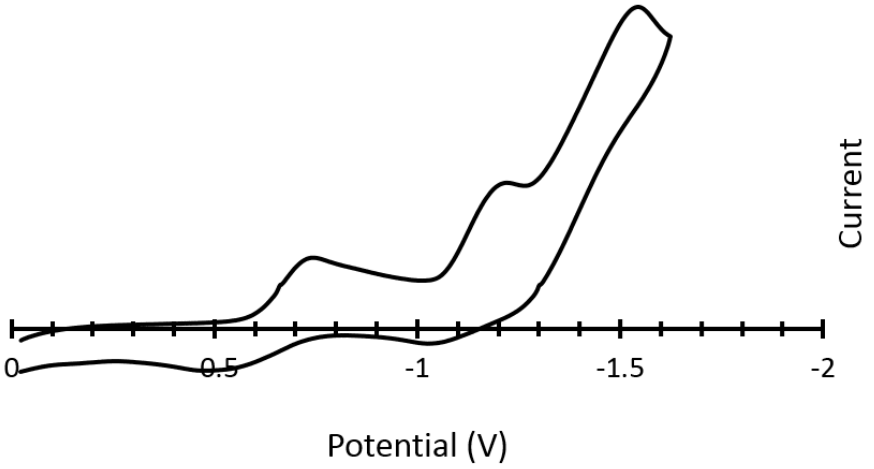

Figure S12. CV of **2** in a 0.1 M dichloromethane solution of Bu_4NPF_6 referenced to Fc^+/Fc after isoprene and anethole were added and O_2 was bubbled through performed at 100mV/s. The scans were all started at the rest potential of the cell (-0.0417 V) and swept cathodically.

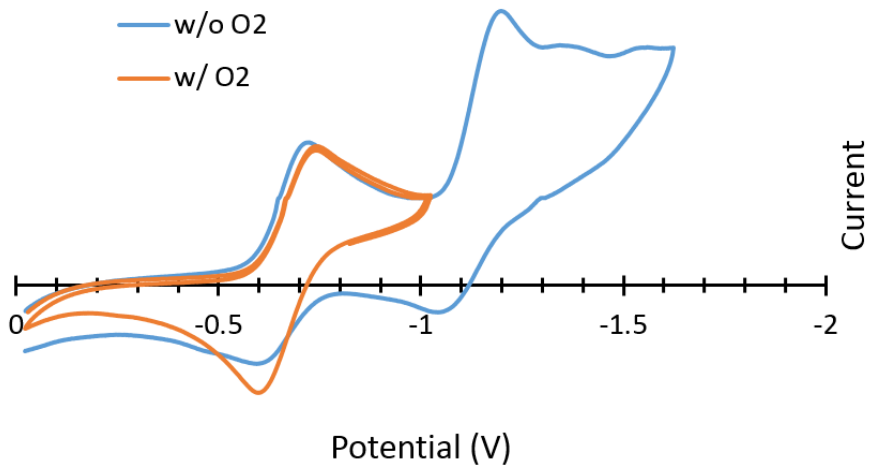

Figure S13. CVs of **2** in a 0.1 M dichloromethane solution of Bu_4NPF_6 referenced to Fc^+/Fc after isoprene and anethole were added performed at 100mV/s. The scans were all started at the rest potential of the cell (-0.0277 V) and swept cathodically.

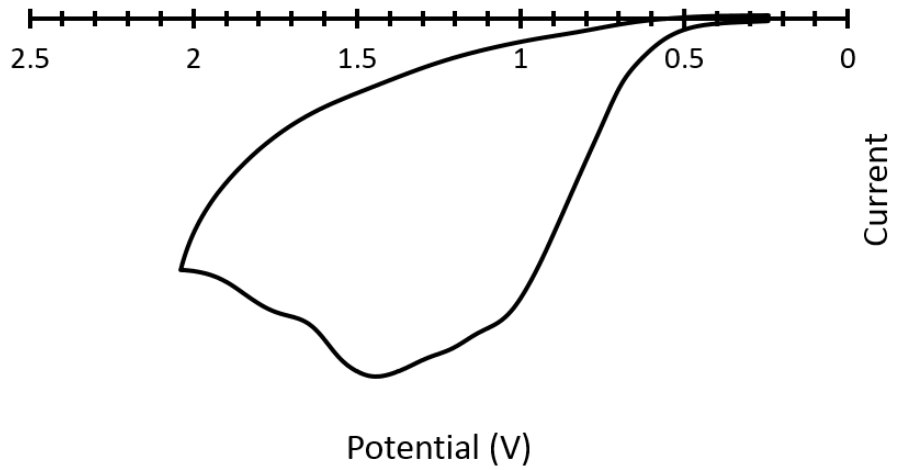

Figure S14. CV of *para*-anethole in a 0.1 M nitromethane solution of Bu_4NPF_6 referenced to Fc^+/Fc in performed at 250 mV/s. The scan was all started at the rest potential of the cell (+0.2480 V) and swept anodically.

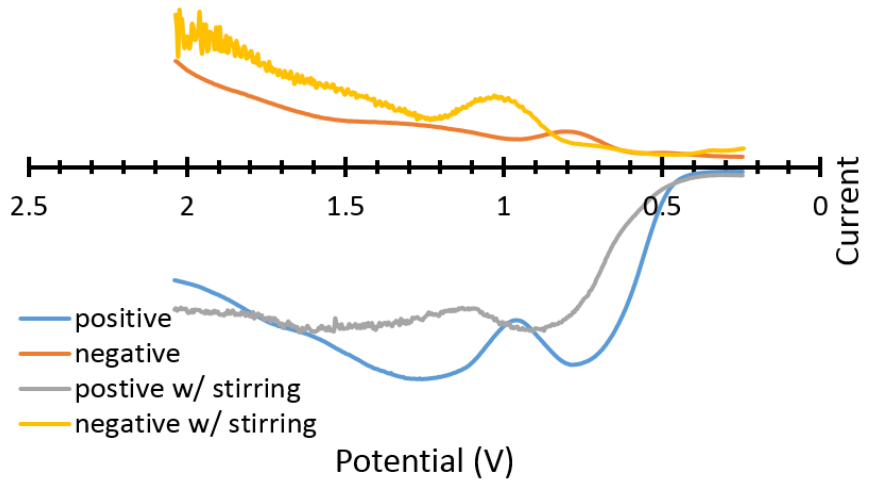

Figure S15. SWVs of *para*-anethole in a 0.1 M nitromethane solution of Bu_4NPF_6 referenced to Fc^+/Fc where the designations negative and positive indicate the step-direction. Each voltammogram was begun at either the most anodic or cathodic potential, dependending on the scan direction.

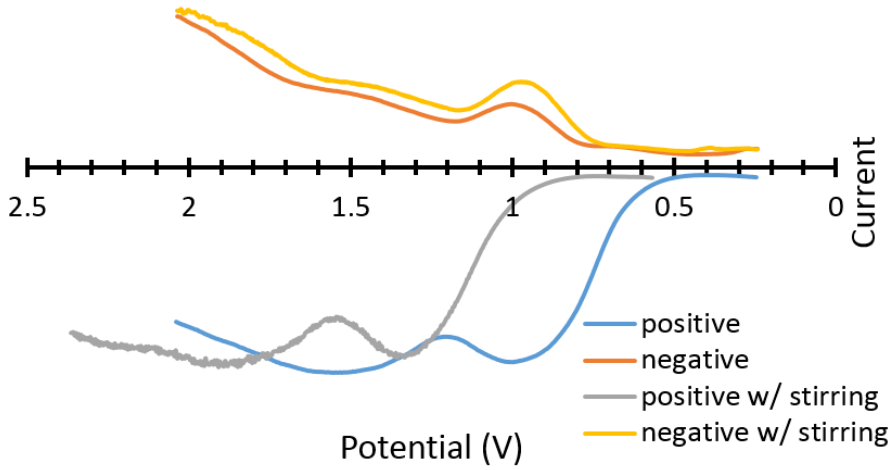

Figure S16. SWVs of *para*-anethole in a 0.1 M nitromethane solution of Bu_4NPF_6 referenced to Fc^+/Fc with O_2 bubbled through where the designations negative and positive indicate the step-direction. Each voltammogram was begun at either the most anodic or cathodic potential, depending on the scan direction.

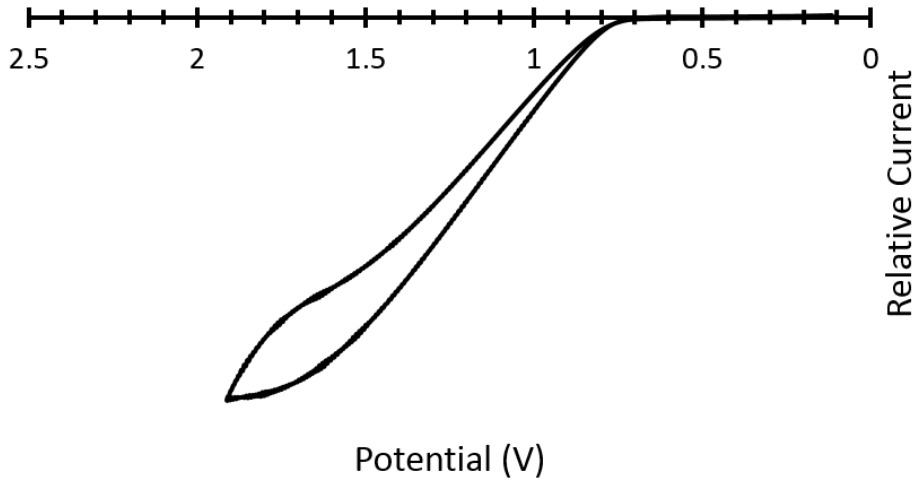

Figure S17. CV of *para*-anethole in a 0.1 M acetonitrile solution of Bu_4NPF_6 referenced to Fc^+/Fc in performed at 250 mV/s. The scan was all started at the rest potential of the cell (+0.1144 V) and swept anodically.

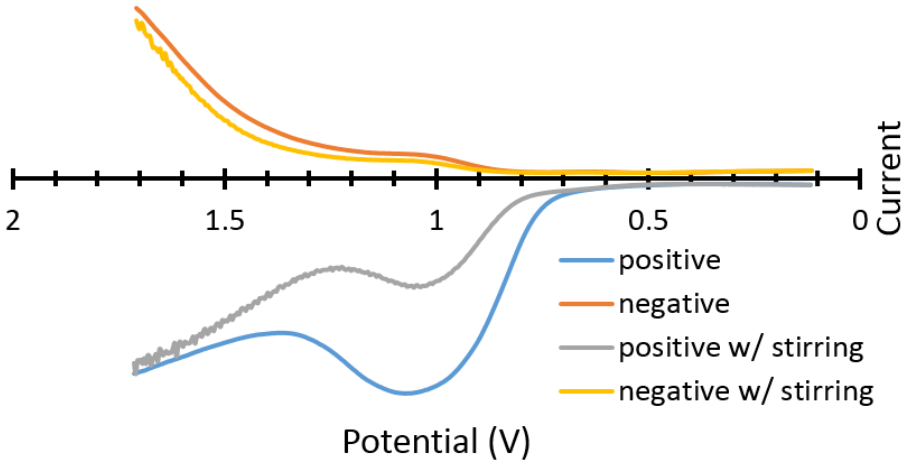

Figure S18. SWVs of *para*-anethole in a 0.1 M acetonitrile solution of Bu_4NPF_6 referenced to Fc^+/Fc where the designations negative and positive indicate the step-direction. Each voltammogram was begun at either the most anodic or cathodic potential, depending on the scan direction.

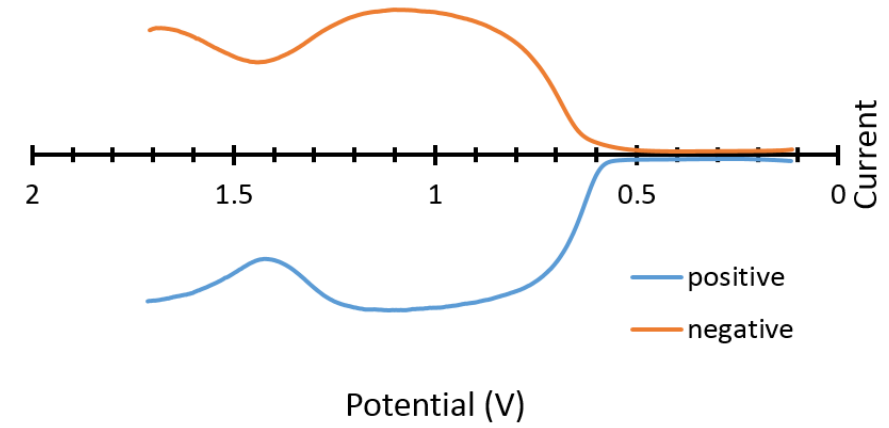

Figure S19. SWVs of *para*-anethole in a 0.1 M acetonitrile solution of Bu_4NPF_6 referenced to Fc^+/Fc with O_2 bubbled through where the designations negative and positive indicate the step-direction. Each voltammogram was begun at either the most anodic or cathodic potential, depending on the scan direction.

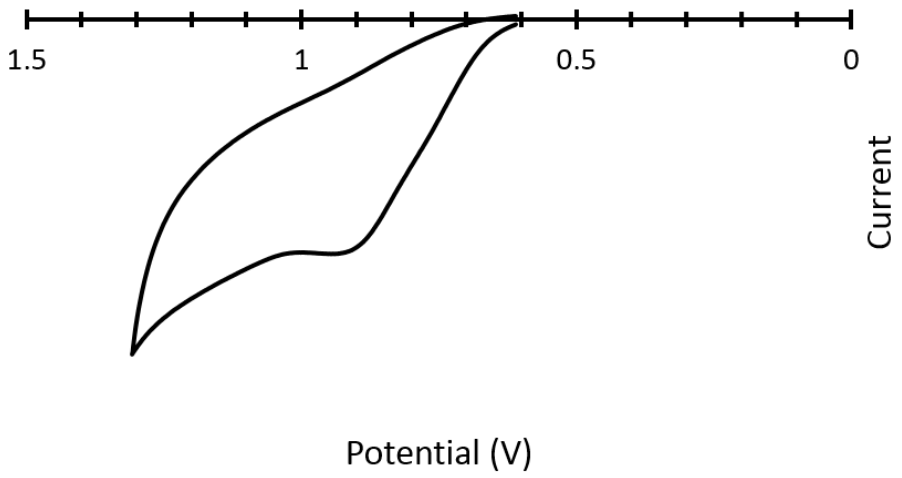

Figure S20. CV of *ortho*-anethole in a 0.1 M nitromethane solution of Bu_4NPF_6 referenced to Fc^+/Fc in performed at 100 mV/s. The scan was all started at the rest potential of the cell (+0.6097 V) and swept anodically.

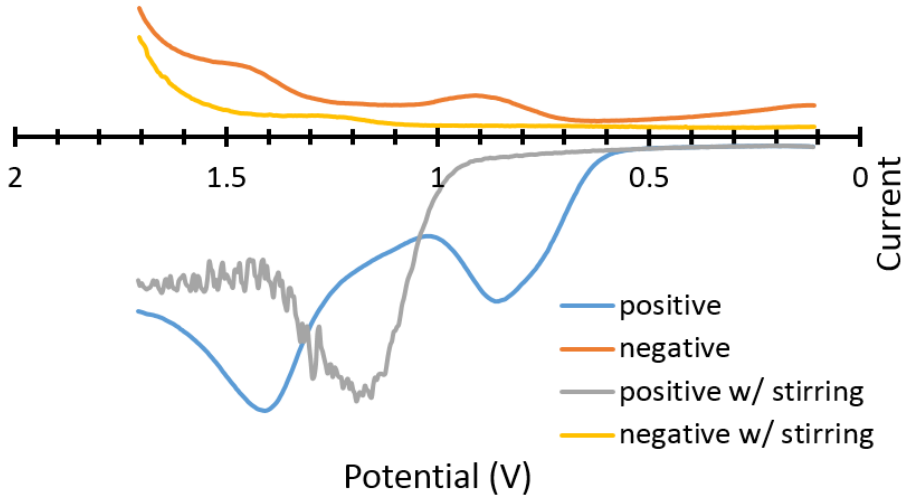

Figure S21. SWVs of *ortho*-anethole in a 0.1 M nitromethane solution of Bu_4NPF_6 referenced to Fc^+/Fc where the designations negative and positive indicate the step-direction. Each voltammogram was begun at either the most anodic or cathodic potential, depending on the scan direction.

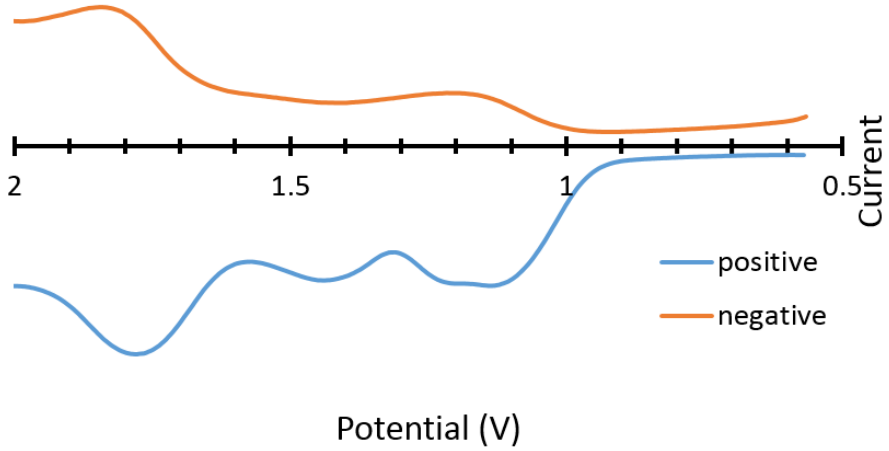

Figure S22. SWVs of *ortho*-anethole in a 0.1 M nitromethane solution of Bu_4NPF_6 referenced to Fc^+/Fc with O_2 bubbled through where the designations negative and positive indicate the step-direction. Each voltammogram was begun at either the most anodic or cathodic potential, depending on the scan direction.

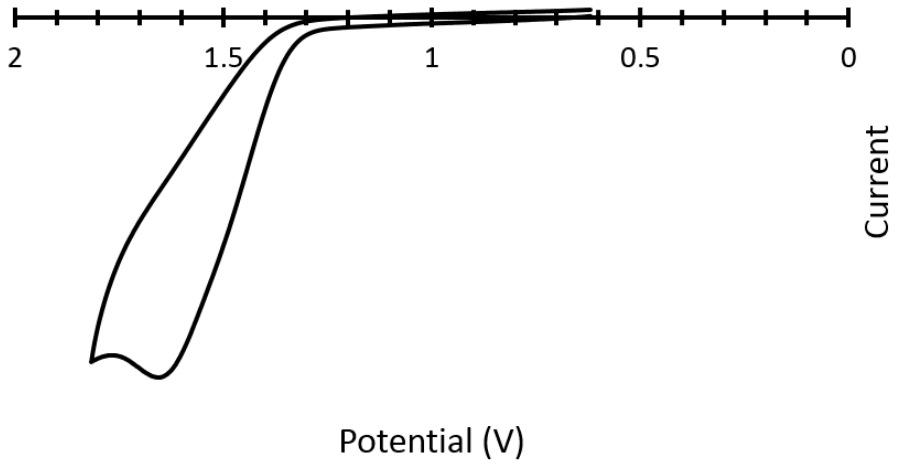

Figure S23. CV of *ortho*-anethole in a 0.1 M acetonitrile solution of Bu_4NPF_6 referenced to Fc^+/Fc in performed at 100 mV/s. The scan was all started at the rest potential of the cell (+0.6186 V) and swept anodically.

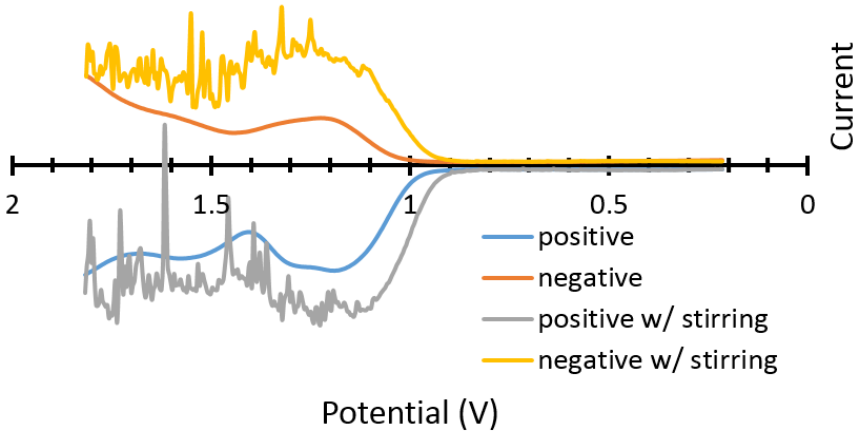

Figure S24. SWVs of *ortho*-anethole in a 0.1 M acetonitrile solution of Bu_4NPF_6 referenced to Fc^+/Fc where the designations negative and positive indicate the step-direction. Each voltammogram was begun at either the most anodic or cathodic potential, depending on the scan direction.

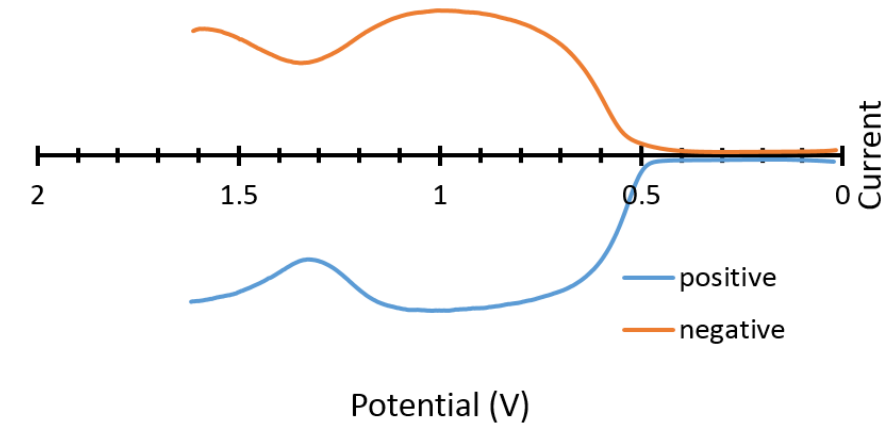

Figure S25. SWVs of *ortho*-anethole in a 0.1 M acetonitrile solution of Bu_4NPF_6 referenced to Fc^+/Fc with O_2 bubbled through where the designations negative and positive indicate the step-direction. Each voltammogram was begun at either the most anodic or cathodic potential, depending on the scan direction.

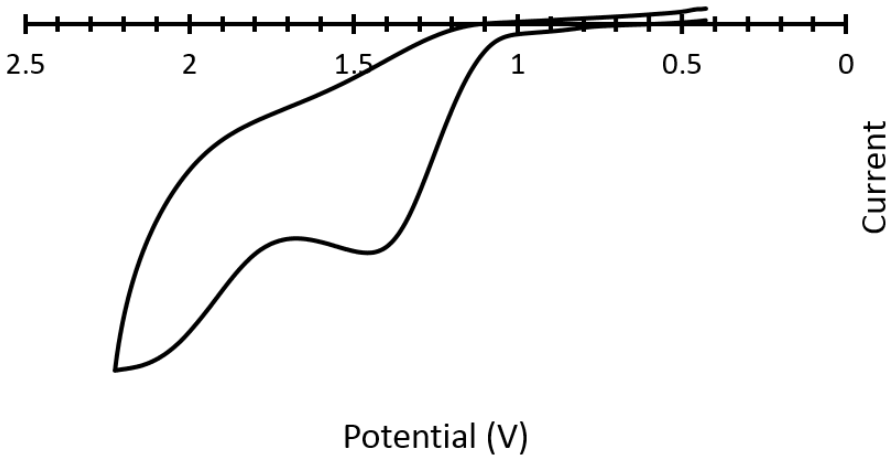

Figure S26. CV of 4'-methoxy-2,4-dimethyl-1,2,3,6-tetrahydro-1,1'-biphenyl in a 0.1 M nitromethane solution of Bu_4NPF_6 referenced to Fc^+/Fc in performed at 100 mV/s. The scan was all started at the rest potential of the cell (+0.4287 V) and swept anodically.

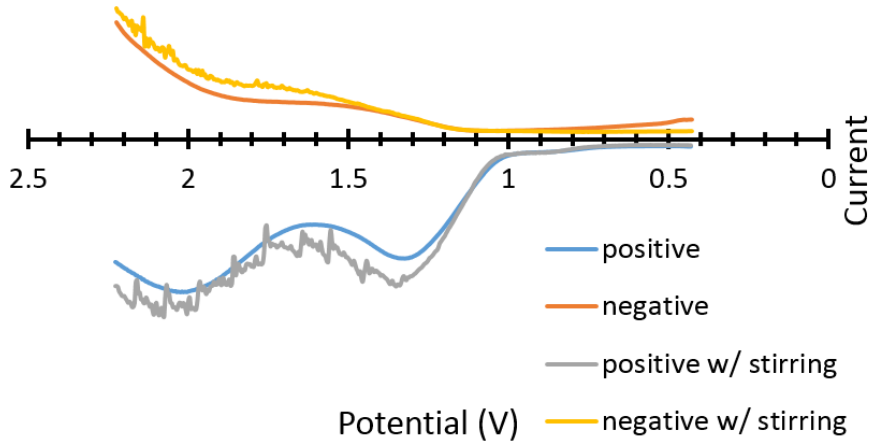

Figure S27. SWVs of 4'-methoxy-2,4-dimethyl-1,2,3,6-tetrahydro-1,1'-biphenyl in a 0.1 M nitromethane solution of Bu_4NPF_6 referenced to Fc^+/Fc where the designations negative and positive indicate the step-direction. Each voltammogram was begun at either the most anodic or cathodic potential, depending on the scan direction.

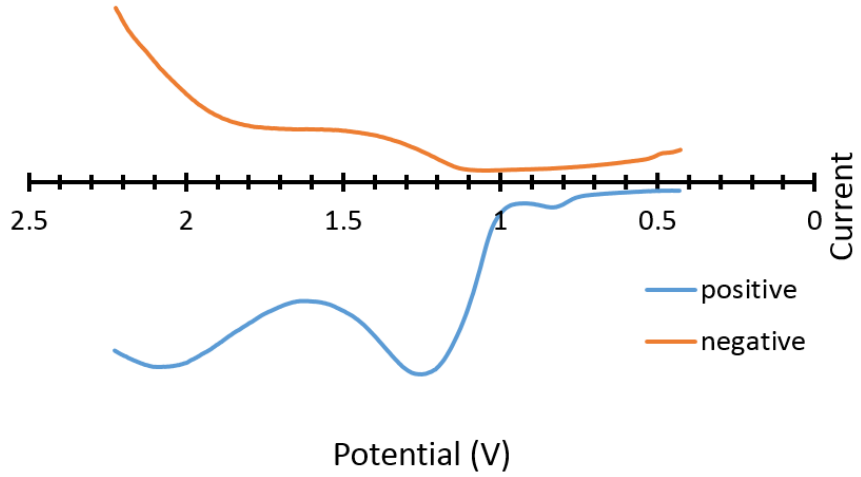

Figure S28. SWVs of 4'-methoxy-2,4-dimethyl-1,2,3,6-tetrahydro-1,1'-biphenyl in a 0.1 M nitromethane solution of Bu_4NPF_6 referenced to Fc^+/Fc with O_2 bubbled through where the designations negative and positive indicate the step-direction. Each voltammogram was begun at either the most anodic or cathodic potential, depending on the scan direction.

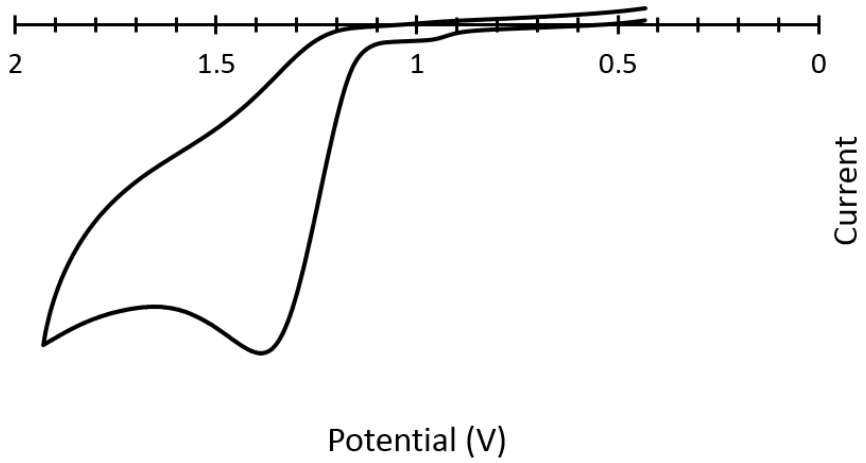

Figure S29. CV of 4'-methoxy-2,4-dimethyl-1,2,3,6-tetrahydro-1,1'-biphenyl in a 0.1 M acetonitrile solution of Bu_4NPF_6 referenced to Fc^+/Fc in performed at 100 mV/s. The scan was all started at the rest potential of the cell (+0.4328 V) and swept anodically.

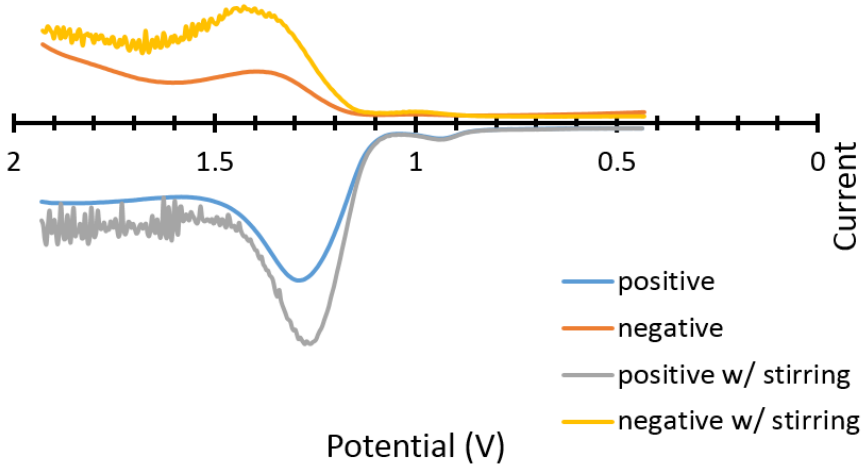

Figure S30. SWVs of 4'-methoxy-2,4-dimethyl-1,2,3,6-tetrahydro-1,1'-biphenyl in a 0.1 M acetonitrile solution of Bu_4NPF_6 referenced to Fc^+/Fc where the designations negative and positive indicate the step-direction. Each voltammogram was begun at either the most anodic or cathodic potential, depending on the scan direction.

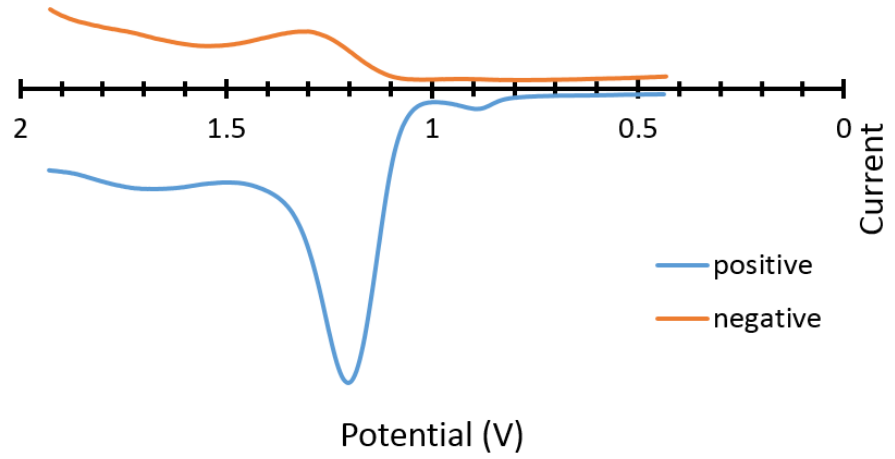

Figure S31. SWVs of 4'-methoxy-2,4-dimethyl-1,2,3,6-tetrahydro-1,1'-biphenyl in a 0.1 M acetonitrile solution of Bu_4NPF_6 referenced to Fc^+/Fc with O_2 bubbled through where the designations negative and positive indicate the step-direction. Each voltammogram was begun at either the most anodic or cathodic potential, depending on the scan direction.

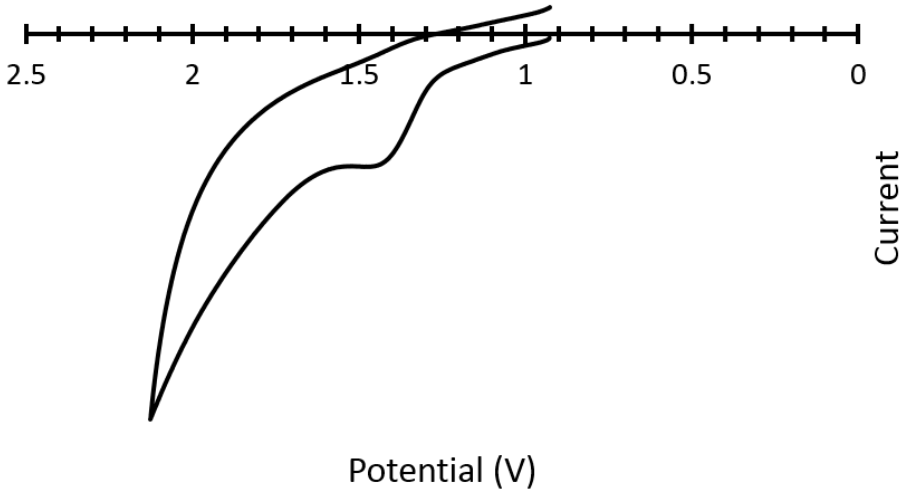

Figure S32. CV of 2'-methoxy-2,4-dimethyl-1,2,3,6-tetrahydro-1,1'-biphenyl in a 0.1 M nitromethane solution of Bu_4NPF_6 referenced to Fc^+/Fc in performed at 250 mV/s. The scan was all started at the rest potential of the cell (+0.9282 V) and swept anodically.

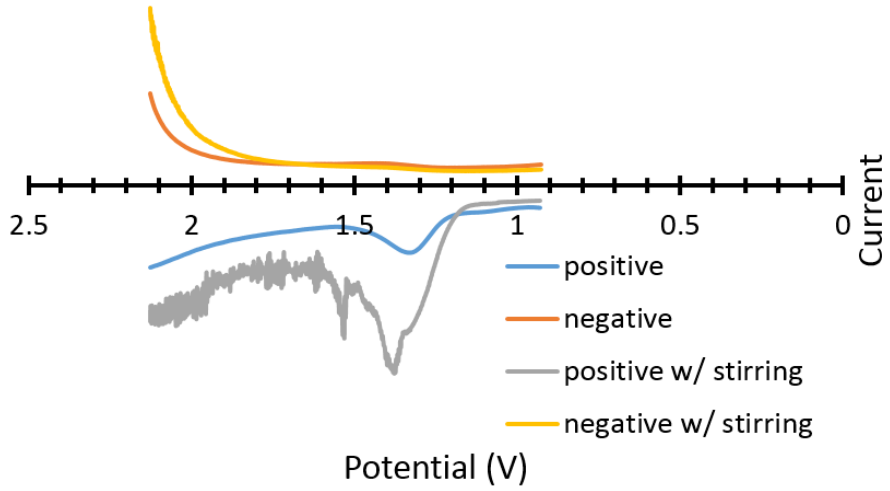

Figure S33. SWVs of 2'-methoxy-2,4-dimethyl-1,2,3,6-tetrahydro-1,1'-biphenyl in a 0.1 M nitromethane solution of Bu_4NPF_6 referenced to Fc^+/Fc where the designations negative and positive indicate the step-direction. Each voltammogram was begun at either the most anodic or cathodic potential, depending on the scan direction.

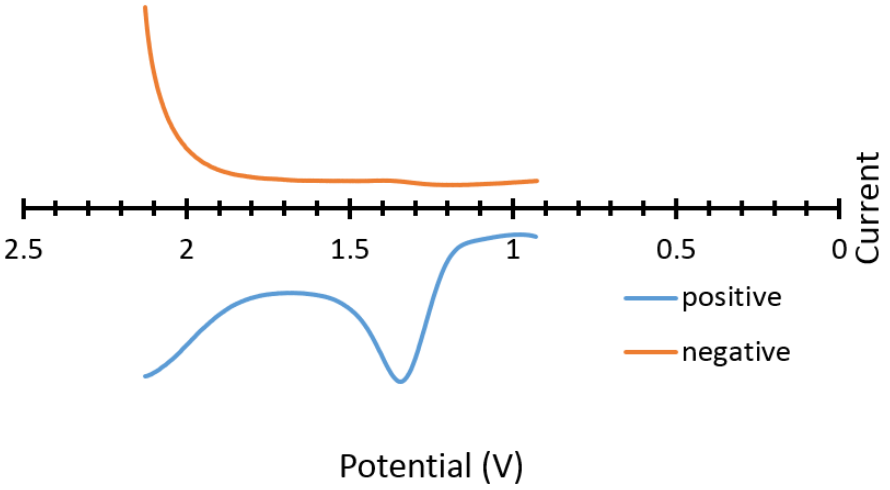

Figure S34. SWVs of 2'-methoxy-2,4-dimethyl-1,2,3,6-tetrahydro-1,1'-biphenyl in a 0.1 M nitromethane solution of Bu_4NPF_6 referenced to Fc^+/Fc with O_2 bubbled through where the designations negative and positive indicate the step-direction. Each voltammogram was begun at either the most anodic or cathodic potential, depending on the scan direction.

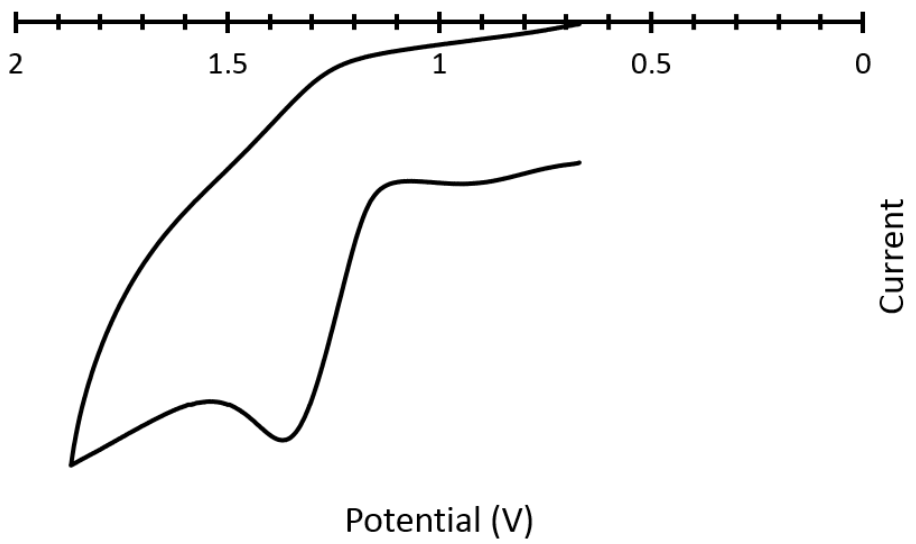

Figure S35. CV of 2'-methoxy-2,4-dimethyl-1,2,3,6-tetrahydro-1,1'-biphenyl in a 0.1 M acetonitrile solution of Bu_4NPF_6 referenced to Fc^+/Fc in performed at 250 mV/s. The scan was all started at the rest potential of the cell (+0.6703 V) and swept anodically.

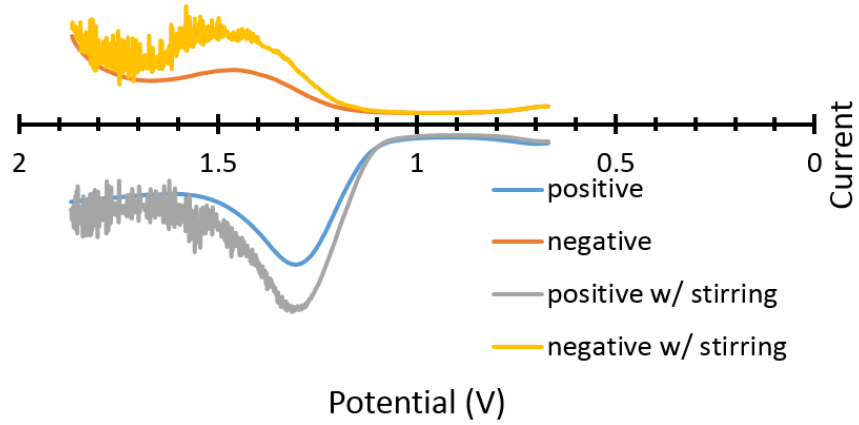

Figure S36. SWVs of 2'-methoxy-2,4-dimethyl-1,2,3,6-tetrahydro-1,1'-biphenyl in a 0.1 M acetonitrile solution of Bu_4NPF_6 referenced to Fc^+/Fc where the designations negative and positive indicate the step-direction. Each voltammogram was begun at either the most anodic or cathodic potential, depending on the scan direction.

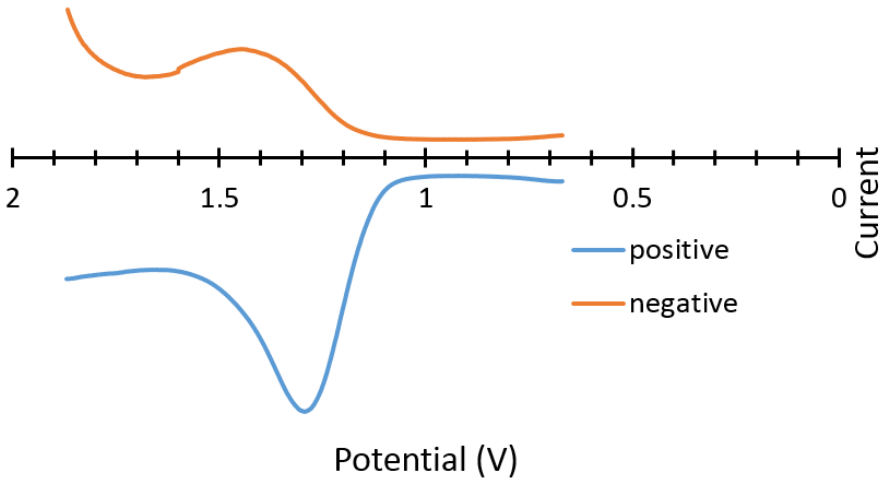

Figure S37. SWVs of 2'-methoxy-2,4-dimethyl-1,2,3,6-tetrahydro-1,1'-biphenyl in a 0.1 M acetonitrile solution of Bu_4NPF_6 referenced to Fc^+/Fc with O_2 bubbled through where the designations negative and positive indicate the step-direction. Each voltammogram was begun at either the most anodic or cathodic potential, depending on the scan direction.

Table S1. Compilation of electrochemical data for $[Ru(bpz)_3]^{2+}$.

conditions	$E_{1/2}$ $[Ru(bpz)_3]^{2+/1+}$	$E_{1/2}$ $[Ru(bpz)_3]^{2*+/1+}$	$E_{1/2}$ $[Cr(Ph_2phen)_3]^{3+/2+}$	$E_{1/2}$ $[Cr(Ph_2phen)_3]^{3*+/2}$
CH_3CN (0.1 M Et_4NOH)[5]	-1.20 ($^{3+/2+}$ +1.46)	+1.02	---	---
CH_3CN (0.1 M Bu_4NPF_6)[6]	-1.17	+0.99	-0.68	+1.00

All $E_{1/2}$ values referenced to Fc^+/Fc and performed at 25 °C under O_2-free conditions.

Electronic Absorption Data for Anethole Oxidation

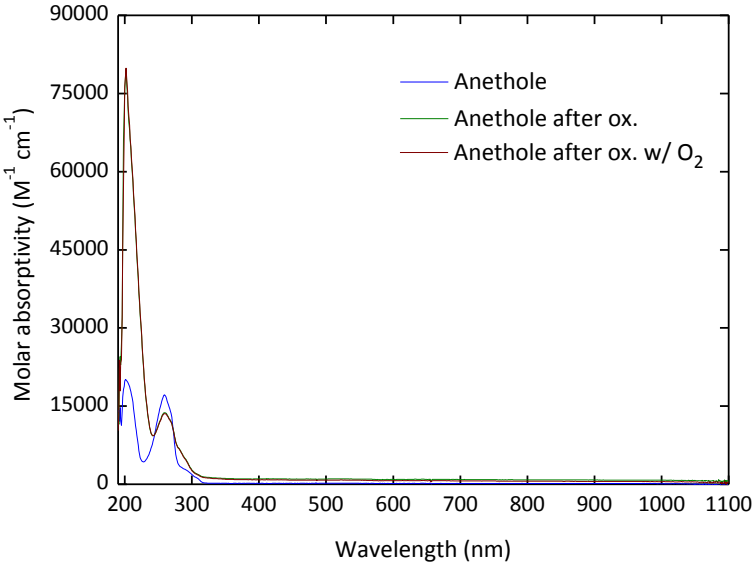

Figure S38. UV-visible spectra of anethole (0.01904 mM) in CH_3CN, after chemical oxidation with cerium ammonium nitrate. The maroon and green traces nearly overlay.

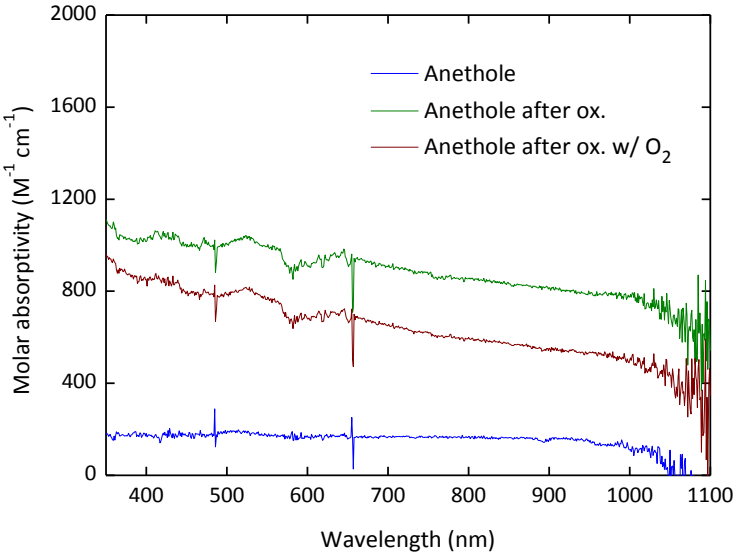

Figure S39. UV-visible spectra of anethole (0.01904 mM) in CH_3CN after chemical oxidation with cerium ammonium nitrate. The changes in the visible region are more evident using a smaller regime of molar absorptivities. The transition at ~550 nm is associated with the anethole radical as evidenced previously.[7]

Spectroelectrochemical Data

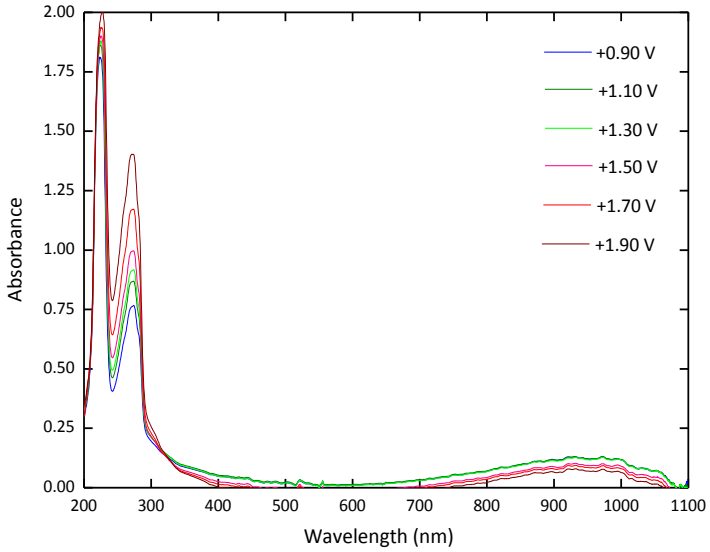

Figure S40. Spectro-electrochemical oxidation of 4'-methoxy-2,4-dimethyl-1,2,3,6-tetrahydro-1,1'-biphenyl in CH_3CN (0.1 M Bu_4NPF_6) where all potentials are referenced vs. Fc^+/Fc.

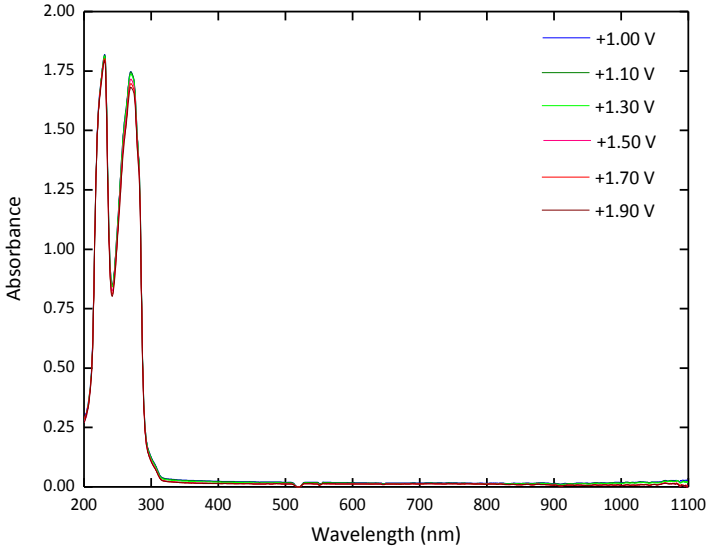

Figure S41. Spectro-electrochemical oxidation of 4'-methoxy-2,4-dimethyl-1,2,3,6-tetrahydro-1,1'-biphenyl in CH_3CN (0.1 M Bu_4NPF_6) after exposure to O_2 where all potentials are referenced vs. Fc^+/Fc.

Infrared Spectroscopy for Cr-containing Complexes

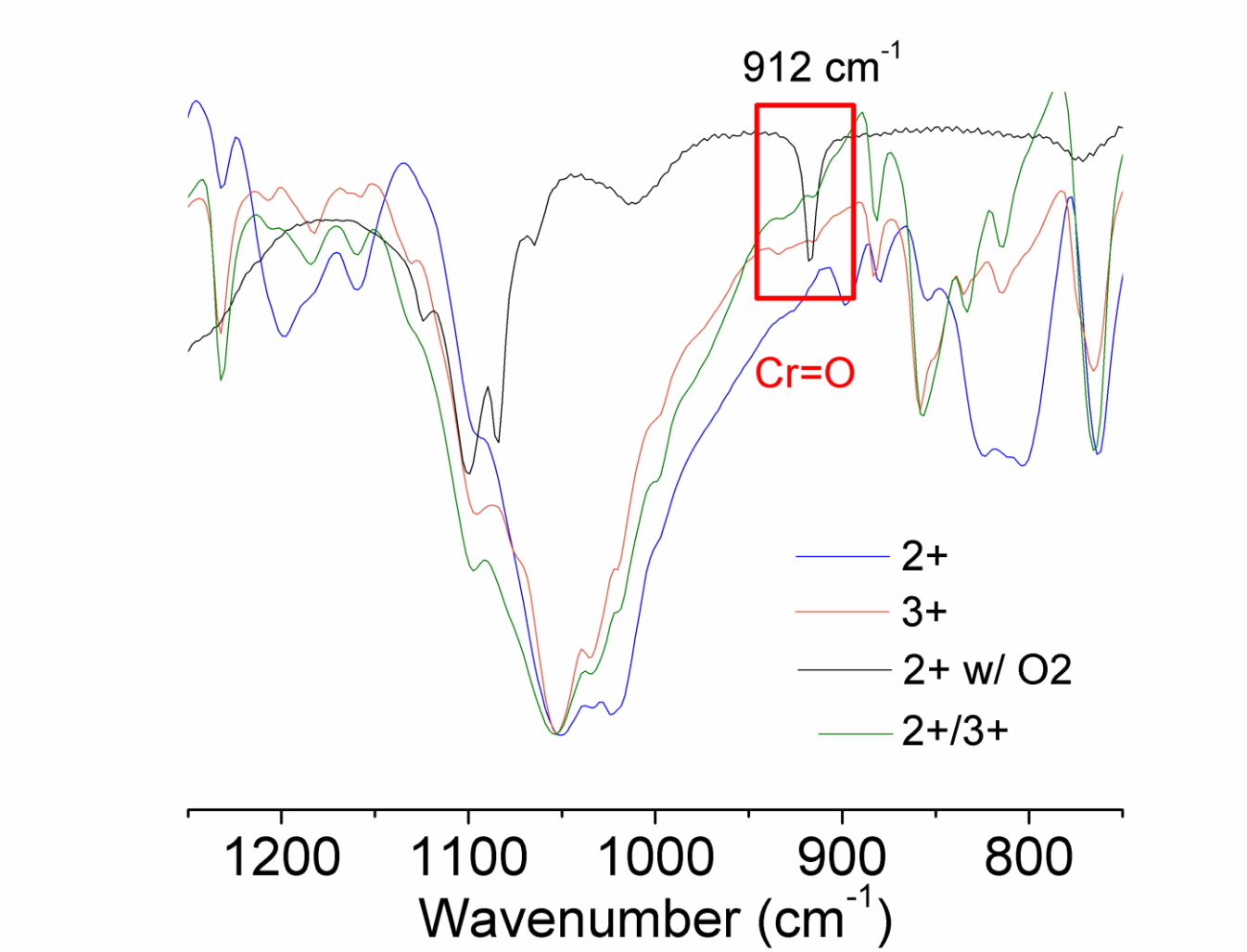

Figure S42. IR spectra of **1** (blue trace), **2** (orange trace), **1** after exposure to O_2 (black trace) and **1** and **2** in degassed CH_3NO_2 irradiated for 20 minutes and then exposed to air for 30 minutes (green trace). The black trace was gathered after a solution of **1** in CH_3CN had O_2 bubbled through for 10 seconds. The green trace was exposed to air via a needle air outlet and the solvent was removed before the IR was gathered.

Electronic Absorption of Chromyl Species

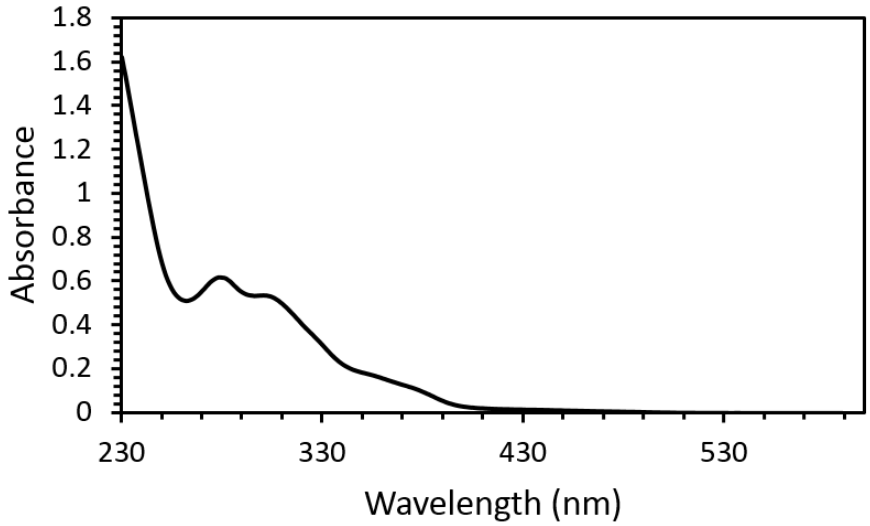

Figure S43. Electronic absorption spectrum of species formed when a CH_3CN solution of **1** was subjected to bubbling O_2. We do not report molar absorptivities because we do not know the amount present; also, some 4,7-diphenyl-1,10-phenanthroline (Ph_2phen) may be present in solution. Full decomposition of **1** was observed.

NMR Spectra of Reaction Monitoring Superoxide via Diphenyl Disulfide Formatio

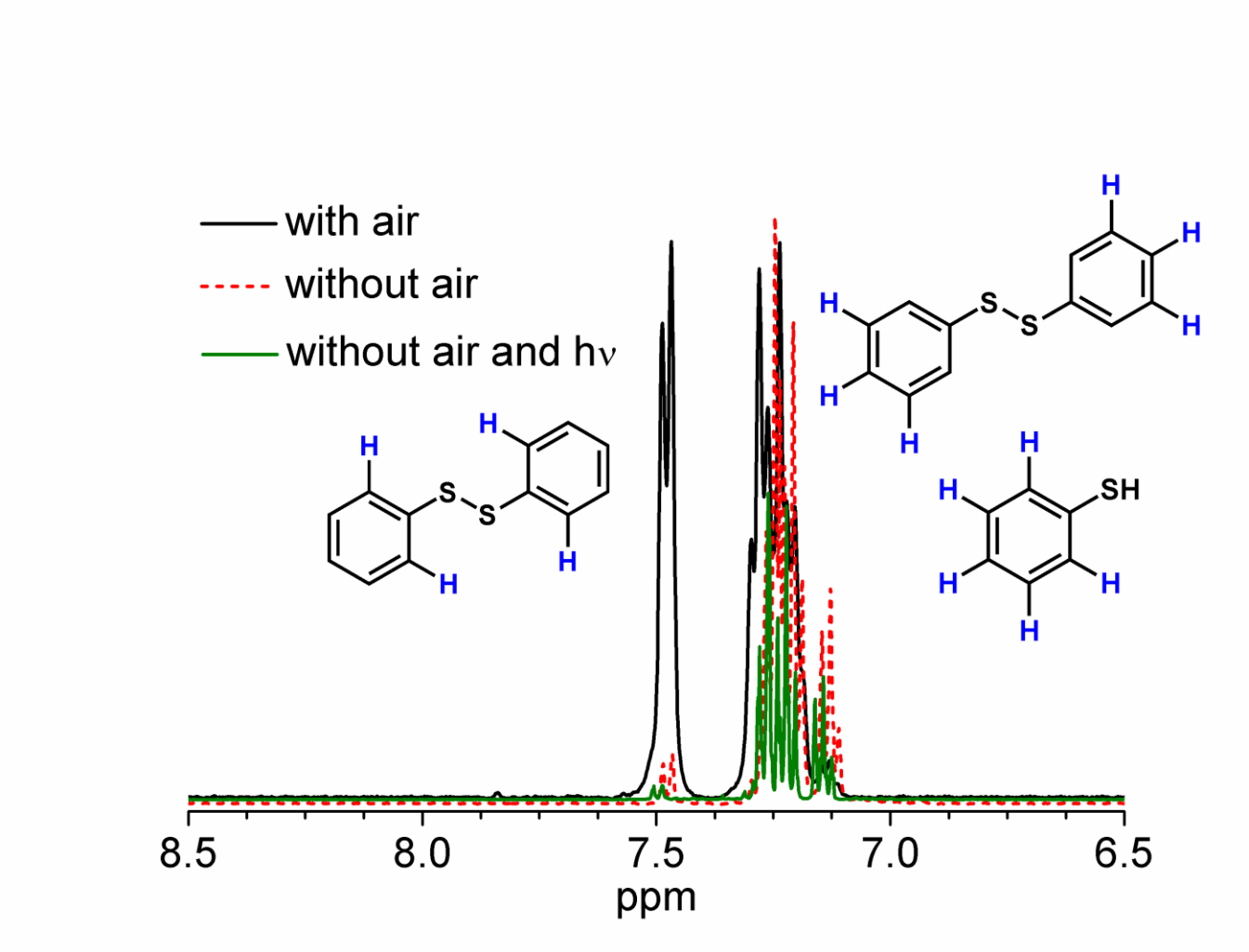

Figure S44. Aromatic region of ^{1}H NMR spectra of experiments where thiophenol spiked into a solution of 3:1 (mol %) **1**:**2** exposed to air (black trace) and a solution of **2** air-free (red trace) after 30 minutes of irradiation (419, 350 and 300 nm sources) and a solution of **1**:**3** kept air and light free (green trace). The spectra were referenced to $CDCl_3$. The blue protons are represent the peaks of interest for both diphenyl disulfide and thiophenol. The green trace gave integrations showing less than 2% conversion to diphenyl disulfide.

Fit Parameters for Quenching Studies

Table S2. Values obtained from fitting time-resolved emission data to a single exponential decay function for the deoxygenated sample of $[Cr(Ph_2phen)_3]^{3+}$ with *para*-anethole as the quencher.

[Quencher] / mM	τ / ns
0	441000 ± 900
1.09	949 ± 1
2.11	497.6 ± 0.6
3.07	340.9 ± 0.5
4.81	220.3 ± 0.4

Table S3. Values obtained from fitting time-resolved emission data to a single exponential decay function for the ambient oxygen sample of $[Cr(Ph_2phen)_3]^{3+}$ with *para*-anethole as the quencher.

[Quencher] / mM	τ / ns
0	13415 ± 9
0.87	1002.5 ± 0.9
1.69	574.8 ± 0.6
2.45	403.3 ± 0.5
3.86	266.0 ± 0.4

Time Dependent Electronic Absorption Data

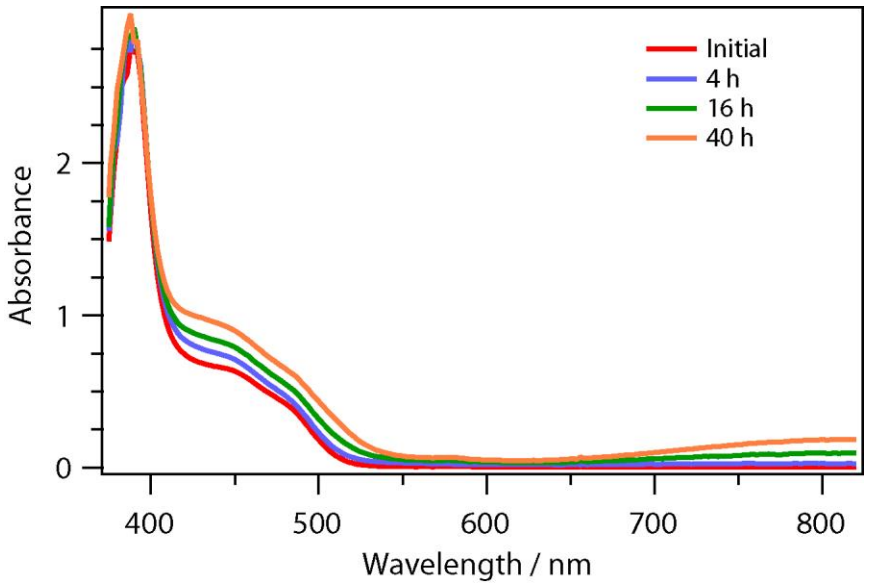

Figure S45. Electronic absorption spectra taken at the indicated time points of the deoxygenated reaction mixture. Experimental the same as in **Cyclohexene** 5 above using a Teflon-sealed 1 cm × 1 cm quartz cuvette, an Ecosmart Bright White 100 W replacement CFL (120 V, 23 W, 3500 K) at 6 cm for irradiation, diluted to 33%, and bubble degassed with Ar in the dark prior to sealing.

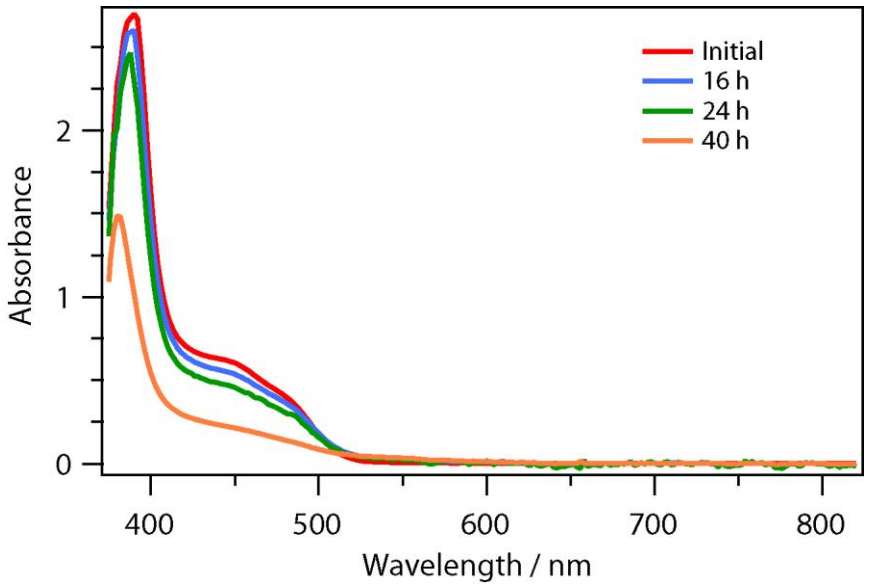

Figure S46. Electronic absorption spectra taken at the indicated time points of the ambient oxygen reaction mixture. Experimental the same as in **Cyclohexene 5 Air outlet** above using a 1 cm × 1 cm quartz cuvette, an Ecosmart Bright White 100 W replacement CFL (120 V, 23 W, 3500 K) at 6 cm for irradiation, and diluted to 33%.

Computed Electronic Absorption Data

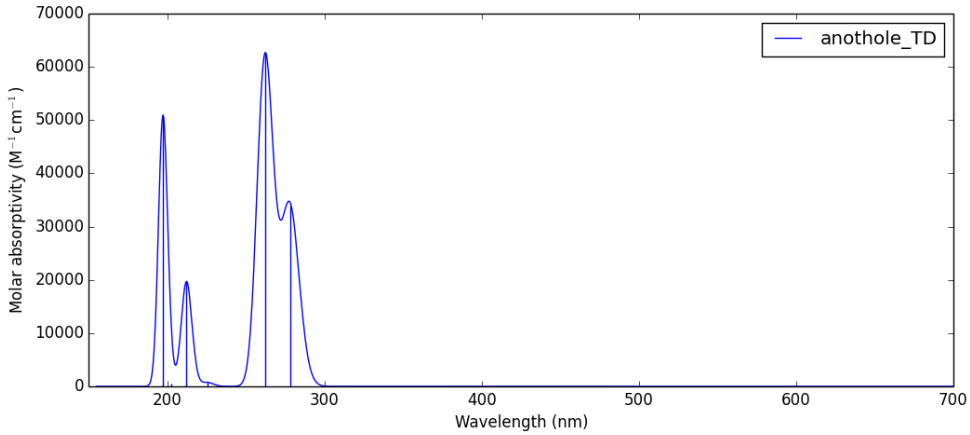

Figure S47. *para*-Anethole **3** TD-DFT spectrum.

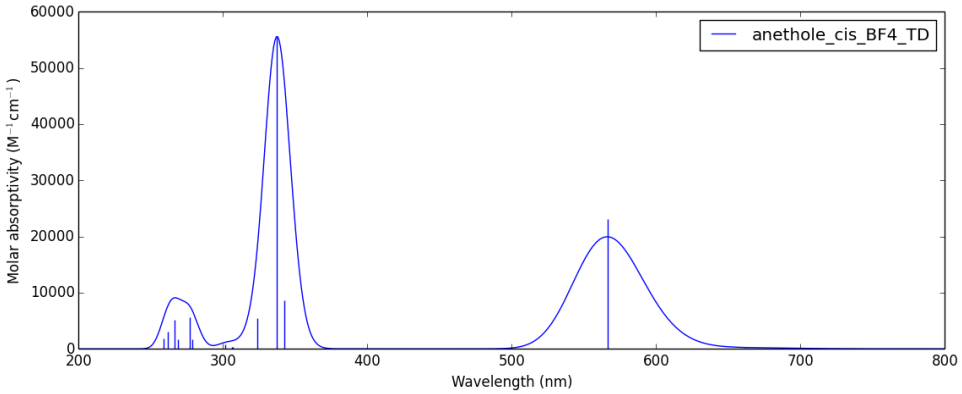

Figure S48. Anethole radical cation·BF_4 TD-DFT spectrum.

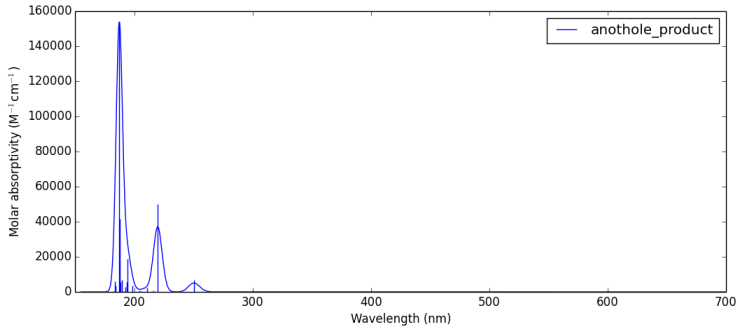

Figure S49. Cycloadduct **5** TD-DFT spectrum.

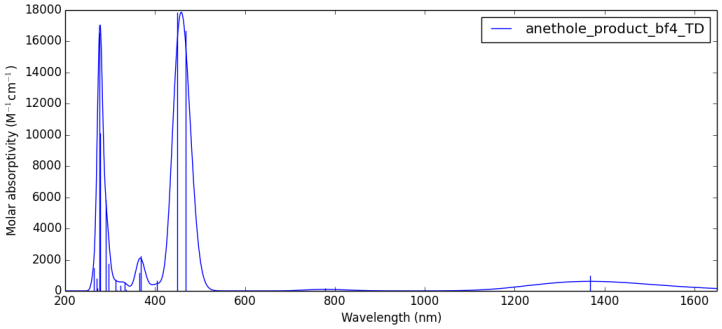

Figure S50. Cycloadduct **5** radical cation·BF_4 TD-DFT spectrum.

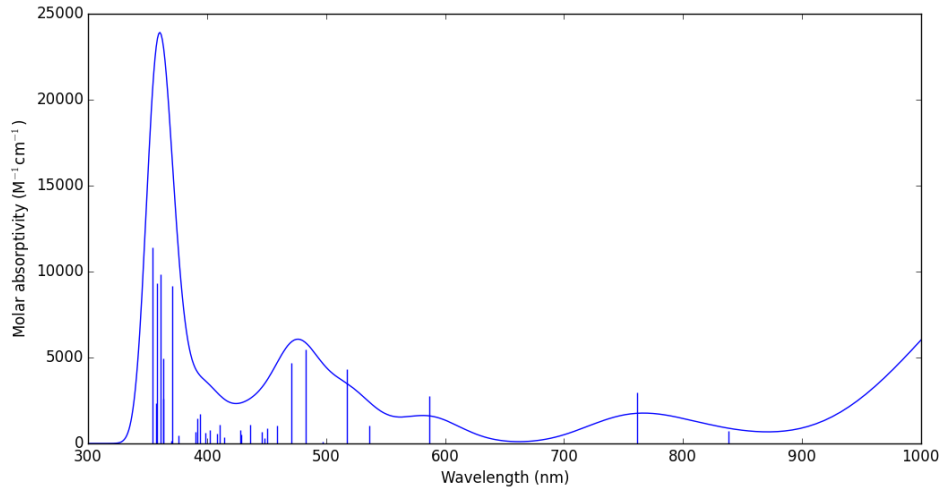

Figure S51. 1·$(BF_4)_2$ TD-DFT spectrum.

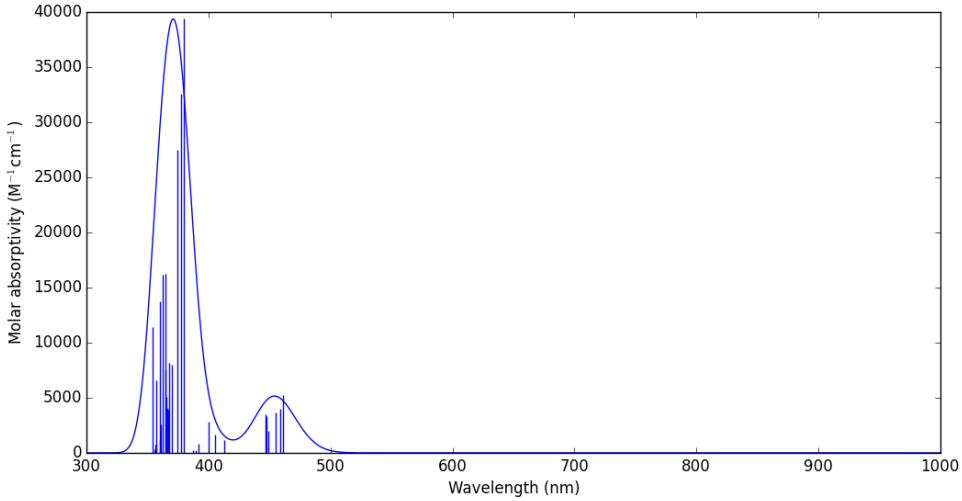

Figure S52. 2·$(BF_4)_2$ TD-DFT spectrum.

Spin Density and Electrostatic Potential Plots

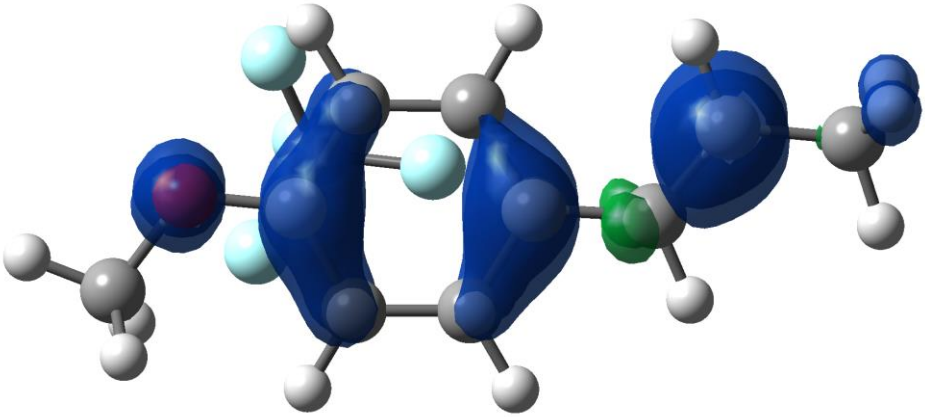

Figure S53. Anethole radical cation·BF_4 net spin density plot. Blue and green shading correspond to α and β spins, respectively; the 0.003 electron density |isovalue| surface is displayed.

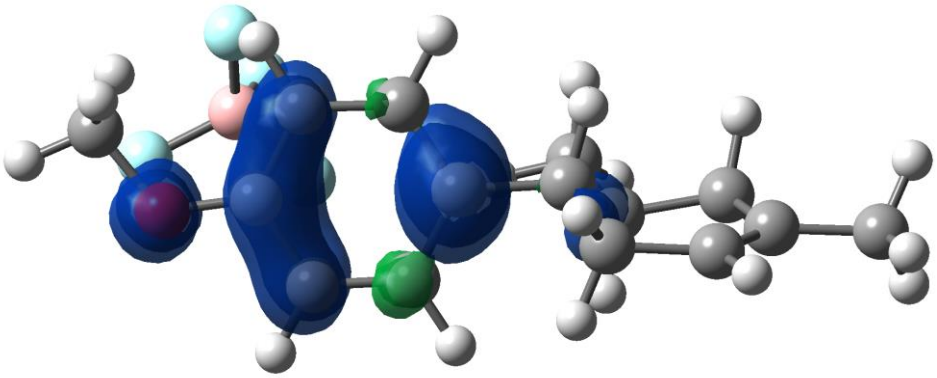

Figure S54. Anethole product radical cation·BF_4 net spin density plot. Blue and green shading correspond to α and β spins, respectively; the 0.003 electron density |isovalue| surface is displayed.

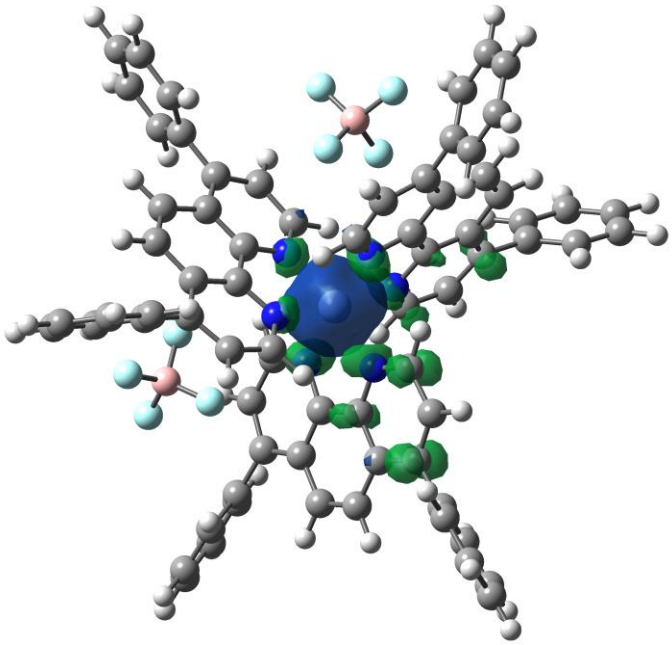

Figure S55. Spin density plots generated from APFD calculations for the cationic complex based on the structure of 1. Blue and green shading correspond to α and β spins, respectively; the 0.003 electron density |isovalue| surface is displayed.

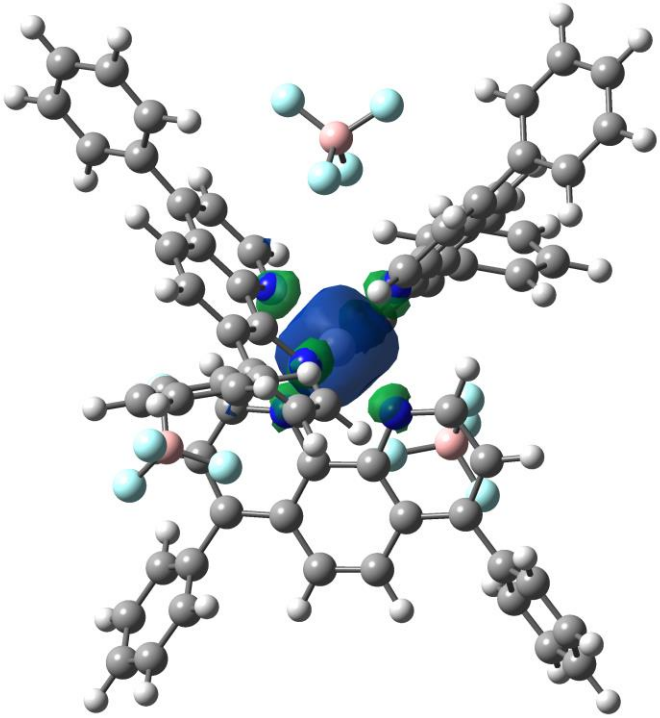

Figure S56. Spin density plots generated from APFD calculations for the cationic complex based on the structure of 2. Blue and green shading correspond to α and β spins, respectively; the 0.003 electron density |isovalue| surface is displayed.

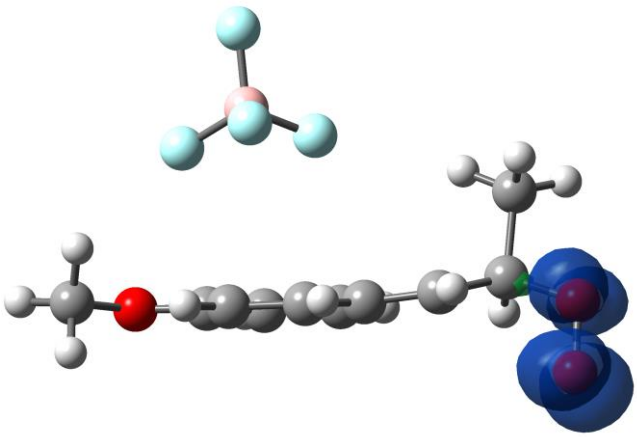

Figure S57. Superoxo isomer of O_2·anethole radical cation·BF_4 net spin density plot. Blue and green shading correspond to α and β spins, respectively; the 0.003 electron density |isovalue| surface is displayed.

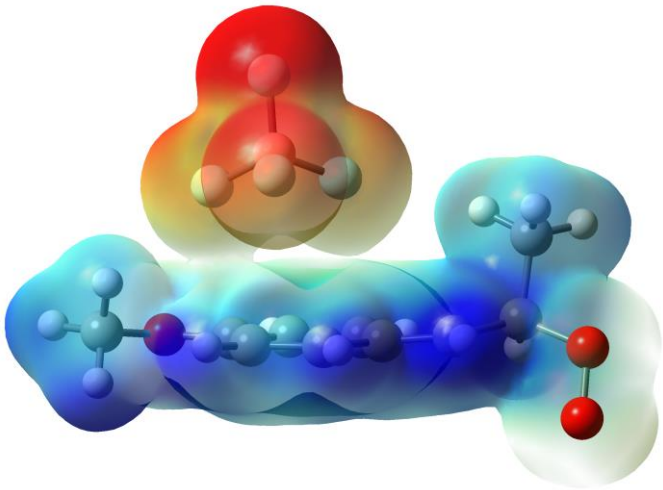

Figure S58. Side view of the superoxo isomer of O_2·anethole radical cation·BF_4 electrostatic potential mapped onto the total density plot. The 0.08 electron density |isovalue| surface is displayed and the electrostatic potential is mapped onto the range from -0.12 to 0.12.

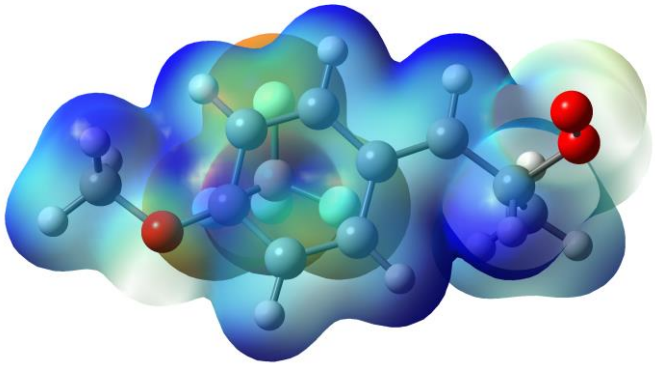

Figure S59. Bottom view of the superoxo isomer of O_2·anethole radical cation·BF_4 electrostatic potential mapped onto the total density plot. The 0.08 electron density |isovalue| surface is displayed and the electrostatic potential is mapped onto the range from -0.12 to 0.12.

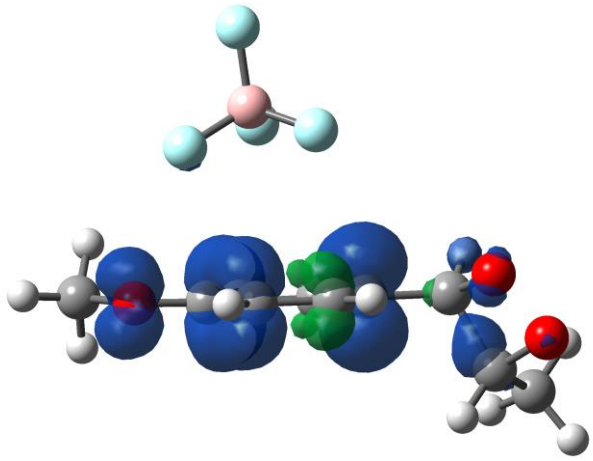

Figure S60. Dioxetane isomer of O_2·anethole radical cation·BF_4 net spin density plot. Blue and green shading correspond to α and β spins, respectively; the 0.003 electron density |isovalue| surface is displayed.

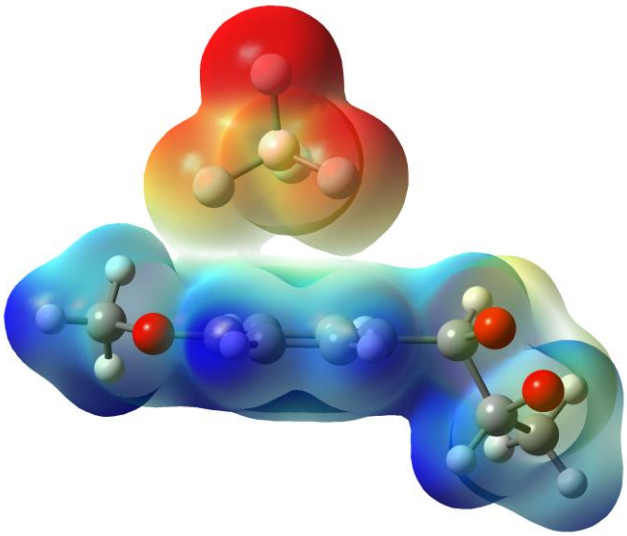

Figure S61. Side view of the dioxetane isomer of O_2·anethole radical cation·BF_4 electrostatic potential mapped onto the total density plot. The 0.08 electron density |isovalue| surface is displayed and the electrostatic potential is mapped onto the range from -0.12 to 0.12.

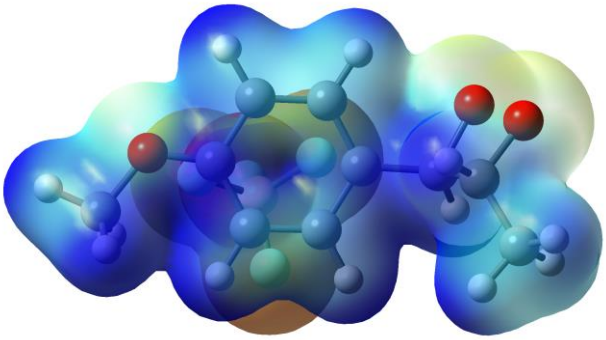

Figure S62. Bottom view of the dioxetane isomer of O_2·anethole radical cation·BF_4 electrostatic potential mapped onto the total density plot. The 0.08 electron density |isovalue| surface is displayed and the electrostatic potential is mapped onto the range from -0.12 to 0.12.

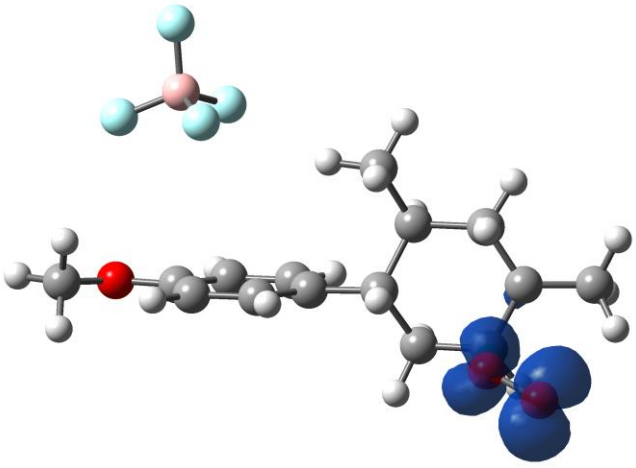

Figure S63. Superoxo isomer of O_2·anethole product (cycloadduct) radical cation·BF_4 net spin density plot. Blue and green shading correspond to α and β spins, respectively; the 0.003 electron density |isovalue| surface is displayed.

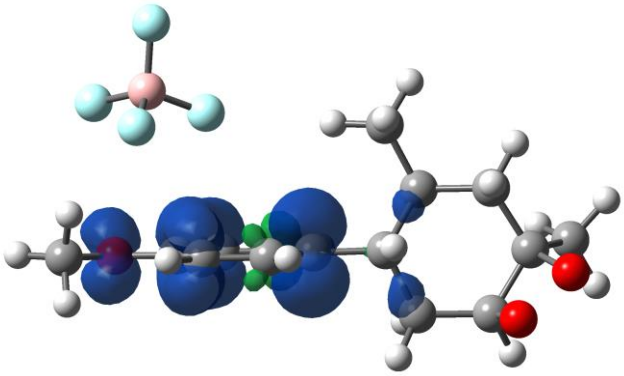

Figure S65. Dioxetane isomer of O_2·anethole product (cycloadduct) radical cation·BF_4 net spin density plot. Blue and green shading correspond to α and β spins, respectively; the 0.003 electron density |isovalue| surface is displayed.

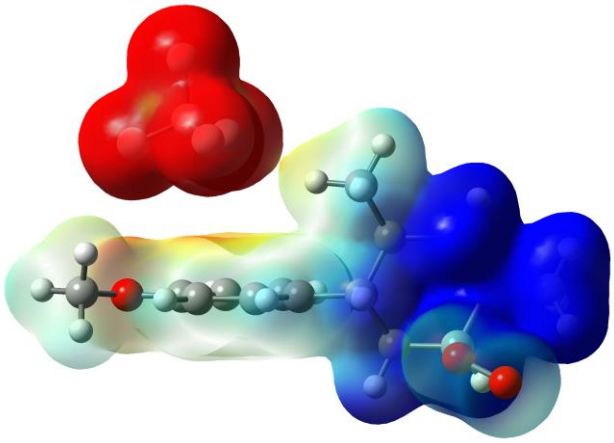

Figure S64. Side view of the superoxo isomer of O_2·anethole product (cycloadduct) radical cation·BF_4 electrostatic potential mapped onto the total density plot. The 0.08 electron density |isovalue| surface is displayed and the electrostatic potential is mapped onto the range from -0.12 to 0.12.

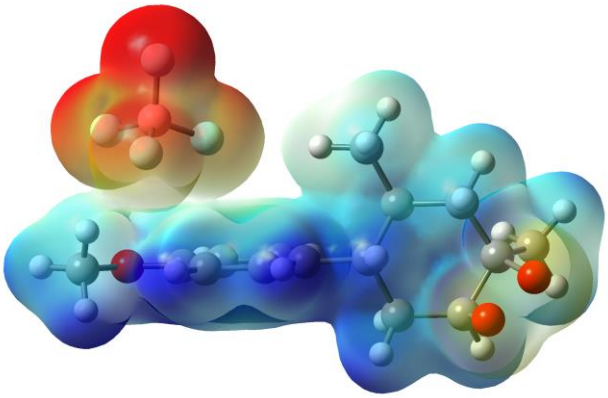

Figure S66. Side view of the dioxetane isomer of O_2·anethole product (cycloadduct) radical cation·BF_4 electrostatic potential mapped onto the total density plot. The 0.08 electron density |isovalue| surface is displayed and the electrostatic potential is mapped onto the range from -0.12 to 0.12.

Tabulated Energies for Computed Species

Table S4. Total energies, enthalpies, and entropies (hartree)

Complex	Total Energy	+ Enthalpic corrections	+ Entropic corrections
$^3O_2$ αα	-150.253868894	-150.246688	-150.269942
$^3O_2$ no solvent	-150.253661326	-150.246482	-150.269738
$^2O_2^-$	-150.379271947	-150.373137	-150.396221
$^2O_2^-$ no solvent	-150.266357315	-150.260254	-150.283343
$^1O_2$ αβ	-150.237177424		
$O_2 \cdot (CH_3)_4N^+$	-364.495725800	-364.315276	-364.362442
$(CH_3)_4N^+ \cdot BF_4^-$	-638.567765757	-638.3736	-638.429138
para-Anethole, **3**	-463.207482961	-463.001609	-463.050796
3 (*cis*)	-463.204554521	-462.998389	-463.046412
3 no solvent	-463.200998821	-462.994869	-463.044279
$\mathbf{3}^+$	-463.002656456	-462.796365	-462.845858
$\mathbf{3}^+$ no solvent	-462.936957749	-462.730485	-462.779717
Vertical triplet	-463.091260200	-.-	-.-
3(*cis*) rot TS	-463.124840294	-462.924271	-462.973542
3·BF_4	-887.468047263	-887.24041	-887.308419
3·BF_4 (*cis*)	-887.462284430	-887.234388	-887.300972
3·BF_4 rot TS	-887.423365408	-887.198805	-887.265807
cycloadduct **5**	-658.462082515	-658.129569	-658.188903
3·$BF_4 \cdot O_2$ (superoxo)	-1037.729672120	-1037.491477	-1037.564478
3·$BF_4 \cdot O_2$ (dioxetane)	-1037.727157870	-1037.489022	-1037.559753
(**3**·$BF_4)_2$	-1774.987566590	-1774.527057	-1774.636143
(**3**·$BF_4)_2 \cdot O_2$	-1925.261062670	-1924.790659	-1924.908361
5·BF_4	-1082.711426660	-1082.357171	-1082.436145
5 (dioxetane)	-808.746657380	-808.403029	-808.465347
5·$BF_4 \cdot O_2$ (dioxetane)	-1232.994242210	-1232.628847	-1232.710246
5·$BF_4 \cdot O_2$ (superoxo)	-1232.954270510	-1232.592201	-1232.675242
5·$BF_4 \cdot O_2$ (superoxo ts)	-1232.948675540	-1232.588125	-1232.671545
Isoprene, **4**	-195.178129991	-195.057735	-195.092856
4·BF_4	-619.411430926	-619.270351	-619.326334
3·**4**	-658.395100019	-658.067012	-658.134672
3·**4**·BF_4	-1082.661663810	-1082.311357	-1082.39691
3·**4**·BF_4 (ts)	-1082.659525210	-1082.309733	-1082.390117
5·**4**	-853.649824253	-853.194861	-853.274407
5·**4**·BF_4	-1277.906689980	-1277.429779	-1277.524959
$[Cr(bpy)_3](BF_4)_3$ ααα	-3802.794705340	-3802.214016	-3802.353008
$[Cr(bpy)_3](BF_4)_2$ βααα	-3378.468307510	-3377.911811	-3378.034744
$[Cr(Ph_2phen)_3](BF_4)_3$, **2** ααα	-4458.75716590	-.-	-.-
$[Cr(Ph_2phen)_3](BF_4)_2$, **1** βααα	-4034.43386094	-.-	-.-

Table S5. Excited state total energies (hartree)

Complex	Total Energy
$^1O_2$ αβ	-150.237177424
Anethole vertical triplet	-463.091260200
$[Cr(bpy)_3](BF_4)_3$ doublet es (βαα)	-3802.754947212
$[Cr(bpy)_3](BF_4)_2$ quintet es αααα	-3378.446447510
$[Cr(Ph_2phen)_3](BF_4)_3$, **2** Doublet es (βαα)	-4458.71453975
$[Cr(Ph_2phen)_3](BF_4)_2$, **1** Quintet es αααα	-4034.41544126

Table S6. Superoxide Study Energy differences (kcal/mol)

Complex	Total Energy differences	+Enthalpic corrections	+Entropic corrections
$^3O_2$ +e^- -> $^2O_2^-$ no solvent	-7.8 (-7.96 exp)		
3+$^3O_2$ ->**3**$^+$ + $^2O_2^-$ no solvent	157.7	157.3	157.5
3+$^3O_2$ ->**3**$^+$ + $^2O_2^-$	49.8	49.4	49.4
3+$^3O_2$ +TMA·BF_4->$^2O_2$·TMA+^{2}**3**·BF_4	41.0	41.6	49.7

MD-DFT Discussion

As discussed previously, the doublet excited state of the **[Cr]**$^{3+}$ species and the triplet ground state of the **[Cr]**$^{2+}$ species cannot be described by single determinant wave-functions.[8] Instead, linear combinations of determinants are required for accurate representation. If the three active electrons/orbitals of the **[Cr]**$^{3+}$ species are degenerate ($TE_{\beta\alpha\alpha}$= $TE_{\alpha\beta\alpha}$= $TE_{\alpha\alpha\beta}$) or nearly so, then $TE_{\alpha\alpha\alpha}$-$TE_{\beta\alpha\alpha}$ can be used to estimate the doublet energy, see Equation S.1:

$$TE_{doublet}=TE_{\alpha\alpha\alpha}+3/2(TE_{\beta\alpha\alpha}-TE_{\alpha\alpha\alpha}) \quad (S.1)$$

For the **[Cr]**$^{2+}$ species, where the three d electrons are high-spin (ferromagnetically) coupled and the fourth ligand-based electron is anti-ferromagnetically coupled to form a triplet, the corresponding energy expression is given in Equation S.2:

$$TE_{triplet}=TE_{\beta\alpha\alpha\alpha}-4/3(TE_{\beta\alpha\alpha\alpha}-TE_{\alpha\alpha\alpha\alpha}) \quad (S.2)$$

Unless otherwise noted, all computational results were obtained for neutral species. This ion pair formulation was used to minimize the impact of implicit solvent for ionic species. The APFD and 6-311+g* basis is able to reasonably estimate the electron affinity of $^3O_2$. The computed binding energy is 7.8 kcal/mol whereas the experimental measurement is 8.0 kcal/mol. As the data in Table S5 demonstrate solvation has a very large impact on ionic energetics. For the electron transfer from **3** to $^3O_2$, the gas phase estimate is 158 kcal/mol. In a PCM continuum solvent, the energy drops to 49 kcal/mol. Inclusion of counter ions drops the estimate to 42 kcal/mol. It should be noted at the use of TMA·BF_4 artificially adds an additional particle to the free energy estimate. Free energy data in Table 3 that include TMA·BF_4 have been corrected by this 8.1 kcal/mol entropic factor.

Computed coordinates and parameters

Table S7. Oxygen-related bond distances

$^3O_2$ αα	$R_{O\text{-}O}$=1.19485 Å
$^3O_2$ no solvent	$R_{O\text{-}O}$=1.19528 Å
$^2O_2^-$	$R_{O\text{-}O}$=1.32686 Å
$^2O_2^-$ no solvent	$R_{O\text{-}O}$=1.32958 Å
$^1O_2$ αβ	$R_{O\text{-}O}$=1.19485 Å

Table S8. Computed coordinates: $O_2 \cdot (CH_3)_4N^+$

atom	*Z*	*x*	*y*	*z*
1	7	0.984168	0.012746	0.000280
2	6	2.458903	0.203410	-0.001847
3	6	0.298699	1.339015	0.027278
4	6	0.564364	-0.726066	-1.225851
5	6	0.572168	-0.770979	1.200874
6	1	2.740965	0.772296	-0.886030
7	1	2.747835	0.746193	0.896399
8	1	2.943776	-0.770967	-0.018613
9	1	-0.516324	-0.859392	-1.171628
10	1	0.844378	-0.140754	-2.100258
11	1	1.072731	-1.688973	-1.245375
12	1	0.608424	1.905330	-0.850163
13	1	-0.783894	1.180598	0.021427
14	1	0.604558	1.866830	0.929748
15	1	0.864144	-0.222001	2.094652
16	1	-0.509851	-0.896156	1.152133
17	1	1.074613	-1.736753	1.177470
18	8	-2.809865	0.602464	-0.000848
19	8	-2.433302	-0.667183	0.000292

Table S9. Computed coordinates: $(CH_3)_4N^+ \cdot BF_4^-$

atom	*Z*	*x*	*y*	*z*
1	7	2.008158	0.000101	-0.000128
2	6	3.497727	0.000501	-0.001634
3	6	1.508654	0.945231	1.040985
4	6	1.505852	0.428511	-1.338339
5	6	1.508956	-1.374063	0.298793
6	1	3.851119	1.006555	-0.218850
7	1	3.852174	-0.314397	0.977977
8	1	3.850931	-0.690335	-0.764799
9	1	0.419210	0.423482	-1.321781
10	1	1.875785	1.430884	-1.545955
11	1	1.875176	-0.267545	-2.089152
12	1	1.877860	1.943381	0.812635
13	1	0.421958	0.933597	1.031193
14	1	1.881230	0.623792	2.011752
15	1	1.881518	-1.676166	1.275891
16	1	0.422262	-1.359246	0.297407
17	1	1.878663	-2.053993	-0.466528
18	5	-2.116725	-0.000040	0.000065
19	9	-1.632318	1.296909	-0.273854
20	9	-1.630179	-0.410740	1.259602
21	9	-3.516777	-0.001325	0.000472
22	9	-1.630561	-0.885021	-0.986003

Table S10. Computed coordinates: *para*-Anethole, **3**

atom	*Z*	*x*	*y*	*z*
1	1	-5.311586	0.338495	0.883050
2	1	-5.313189	0.351511	-0.870148
3	1	-4.912075	-1.141738	-0.005012
4	6	-4.789039	-0.055322	0.003013
5	6	-3.349467	0.341683	0.004606
6	1	-3.151894	1.413849	0.013535
7	6	-2.327273	-0.522889	-0.003906
8	1	-2.562970	-1.588553	-0.011637
9	6	-0.895905	-0.210747	-0.003061
10	6	-0.385069	1.099650	-0.003894
11	6	0.031312	-1.256597	-0.001494
12	6	0.975497	1.342403	-0.002303
13	1	-1.062945	1.948250	-0.006394
14	6	1.406865	-1.031027	0.000190
15	1	-0.326862	-2.283589	-0.001293
16	6	1.887920	0.278798	-0.000043
17	1	1.358828	2.358780	-0.003158
18	1	2.082601	-1.878785	0.001581
19	8	3.199463	0.626723	0.001358
20	6	4.164623	-0.410032	0.003169
21	1	5.134767	0.083144	0.004024
22	1	4.075335	-1.034758	0.897552
23	1	4.077495	-1.035898	-0.890631

Table S11. Computed coordinates: **3** (*cis*)

atom	*Z*	*x*	*y*	*z*
1	1	2.707922	-1.367566	1.109421
2	1	3.882175	-1.799970	-0.135638
3	1	4.434561	-1.066047	1.358647
4	6	3.628801	-1.043966	0.618314
5	6	3.509718	0.322018	0.018972
6	1	4.450206	0.851932	-0.131209
7	6	2.389510	0.978835	-0.317863
8	1	2.504592	2.003709	-0.671975
9	6	1.000624	0.510173	-0.236655
10	6	0.619552	-0.822096	-0.468634
11	6	-0.016478	1.427059	0.048832
12	6	-0.704772	-1.218128	-0.382860
13	1	1.367000	-1.555251	-0.753080
14	6	-1.351635	1.045605	0.145503
15	1	0.240326	2.471456	0.210058
16	6	-1.702501	-0.291042	-0.064359
17	1	-0.989849	-2.248987	-0.572495
18	1	-2.100832	1.793853	0.378514
19	8	-2.966281	-0.780779	0.001758
20	6	-4.016402	0.118499	0.310166
21	1	-4.927982	-0.475993	0.315904
22	1	-3.874294	0.572623	1.295901
23	1	-4.102072	0.904732	-0.446612

Table S12. Computed coordinates: **3** no solvent

atom	*Z*	*x*	*y*	*z*
1	1	5.311226	0.346645	-0.876322
2	1	5.310232	0.343526	0.879176
3	1	4.909213	-1.138555	-0.001421
4	6	4.786433	-0.051977	0.000416
5	6	3.346511	0.343025	0.000342
6	1	3.146432	1.414704	0.001044
7	6	2.325498	-0.520577	-0.000365
8	1	2.563594	-1.585822	-0.001018
9	6	0.895072	-0.211863	-0.000314
10	6	0.382768	1.096931	-0.000344
11	6	-0.030030	-1.257166	-0.000245
12	6	-0.976130	1.339385	-0.000229
13	1	1.062046	1.944411	-0.000491
14	6	-1.405077	-1.032547	-0.000121
15	1	0.330180	-2.283591	-0.000265
16	6	-1.886608	0.275818	-0.000098
17	1	-1.365257	2.353135	-0.000261
18	1	-2.080318	-1.881077	-0.000051
19	8	-3.198174	0.625437	-0.000036
20	6	-4.158992	-0.404457	0.000573
21	1	-5.129759	0.088996	0.000850
22	1	-4.074801	-1.032847	-0.893610
23	1	-4.074062	-1.032447	0.894964

Table S13. Computed coordinates: $\mathbf{3}^{+}$

atom	*Z*	*x*	*y*	*z*
1	1	5.246465	0.386577	-0.870650
2	1	5.245639	0.384030	0.873119
3	1	4.882155	-1.126930	-0.001107
4	6	4.737856	-0.045938	0.000356
5	6	3.316617	0.346029	0.000342
6	1	3.109443	1.413730	0.001065
7	6	2.277892	-0.549126	-0.000362
8	1	2.526764	-1.608541	-0.000925
9	6	0.897955	-0.224201	-0.000251
10	6	0.398384	1.114096	-0.000263
11	6	-0.046722	-1.292514	-0.000226
12	6	-0.940942	1.356824	-0.000259
13	1	1.084807	1.952476	-0.000305
14	6	-1.395140	-1.064114	-0.000119
15	1	0.320782	-2.313841	-0.000257
16	6	-1.864158	0.274416	-0.000131
17	1	-1.336670	2.366467	-0.000299
18	1	-2.088254	-1.895988	-0.000145
19	8	-3.129176	0.622759	-0.000154
20	6	-4.161666	-0.373318	0.000629
21	1	-5.093662	0.183627	0.001709
22	1	-4.093068	-0.988006	-0.897734
23	1	-4.091447	-0.988592	0.898464

Table S14. Computed coordinates: $\mathbf{3}^{+}$ no solvent

atom	*Z*	*x*	*y*	*z*
1	1	5.255161	0.392915	-0.870083
2	1	5.253979	0.389013	0.871843
3	1	4.896411	-1.120935	-0.002600
4	6	4.744157	-0.041047	-0.000471
5	6	3.322058	0.345872	-0.000360
6	1	3.111402	1.413993	-0.000174
7	6	2.281293	-0.547611	-0.000071
8	1	2.532192	-1.607219	-0.000086
9	6	0.899800	-0.225279	0.000228
10	6	0.396047	1.111568	0.000454
11	6	-0.044669	-1.294457	0.000426
12	6	-0.943268	1.353596	0.000404
13	1	1.081325	1.951707	0.000713
14	6	-1.393826	-1.068457	0.000473
15	1	0.323606	-2.316248	0.000501
16	6	-1.867088	0.269826	0.000081
17	1	-1.343421	2.361966	0.000527
18	1	-2.086193	-1.901939	0.000932
19	8	-3.128744	0.619281	-0.000316
20	6	-4.173018	-0.364461	-0.000625
21	1	-5.098251	0.204027	-0.001662
22	1	-4.111971	-0.979826	-0.900123
23	1	-4.113205	-0.978998	0.899506

Table S15. Computed coordinates: **3**(*cis*) rot TS

atom	*Z*	*x*	*y*	*z*
1	1	4.673985	0.192236	1.304907
2	1	3.476396	-1.083092	1.424011
3	1	4.919317	-1.318971	0.417909
4	6	4.163417	-0.590634	0.722899
5	6	3.431538	-0.018391	-0.445445
6	1	3.812318	-0.206935	-1.449769
7	6	2.304481	0.887679	-0.260773
8	1	2.507509	1.957214	-0.149573
9	6	0.951175	0.481101	-0.184384
10	6	0.564051	-0.883026	-0.299298
11	6	-0.088342	1.423923	0.013097
12	6	-0.757515	-1.263687	-0.221983
13	1	1.333213	-1.635559	-0.451829
14	6	-1.419112	1.046032	0.091001
15	1	0.166948	2.476780	0.105755
16	6	-1.767335	-0.307284	-0.025826
17	1	-1.042464	-2.308376	-0.310791
18	1	-2.177026	1.806816	0.242076
19	8	-3.032576	-0.791489	0.035497
20	6	-4.093494	0.126476	0.232971
21	1	-5.004769	-0.468192	0.250230
22	1	-3.988625	0.655970	1.185090
23	1	-4.149374	0.850890	-0.585547

Table S16. Computed coordinates: **3**·BF_4

atom	*Z*	*x*	*y*	*z*
1	1	5.510587	1.736695	0.303142
2	1	6.123751	0.109653	0.453434
3	1	5.517406	0.671643	-1.124710
4	6	5.352816	0.708858	-0.047037
5	6	4.009448	0.239136	0.345840
6	1	3.786979	0.248654	1.410517
7	6	3.060978	-0.191810	-0.541095
8	1	3.316654	-0.180876	-1.599119
9	6	1.759161	-0.650645	-0.210957
10	6	1.267196	-0.735685	1.126565
11	6	0.892056	-1.042855	-1.271947
12	6	0.000362	-1.162254	1.374427
13	1	1.900505	-0.453407	1.959352
14	6	-0.383114	-1.471329	-1.039486
15	1	1.258516	-0.986938	-2.292221
16	6	-0.854872	-1.526452	0.297565
17	1	-0.395866	-1.219428	2.381777
18	1	-1.027047	-1.744706	-1.865245
19	8	-2.057544	-1.908404	0.649327
20	6	-3.033153	-2.247903	-0.345316
21	1	-3.935151	-2.485444	0.211096
22	1	-3.202228	-1.391625	-0.996773
23	1	-2.704810	-3.120062	-0.912723
24	5	-1.756159	1.771982	-0.028744
25	9	-1.921381	1.348427	1.303397
26	9	-2.370118	3.027408	-0.204802
27	9	-2.360216	0.832269	-0.894222
28	9	-0.385330	1.870653	-0.327794

Table S17. Computed coordinates: **3**·BF_4 (*cis*)

atom	*Z*	*x*	*y*	*z*
1	1	3.066938	1.273146	1.251295
2	1	4.380004	0.205934	1.765672
3	1	4.759362	1.702733	0.938062
4	6	4.043078	0.879267	0.964509
5	6	4.029457	0.166849	-0.335845
6	1	4.941877	0.242306	-0.924119
7	6	3.013200	-0.542721	-0.927627
8	1	3.200018	-0.863088	-1.950772
9	6	1.733224	-0.882607	-0.418347
10	6	1.364571	-0.822413	0.958525
11	6	0.753883	-1.339269	-1.352751
12	6	0.096837	-1.122516	1.352195
13	1	2.099627	-0.564185	1.708192
14	6	-0.526167	-1.623735	-0.976969
15	1	1.033215	-1.425642	-2.398211
16	6	-0.881968	-1.495941	0.390683
17	1	-0.201734	-1.077566	2.393315
18	1	-1.258255	-1.926111	-1.714663
19	8	-2.077019	-1.723201	0.875919
20	6	-3.163603	-2.061086	0.003244
21	1	-4.030023	-2.154414	0.651400
22	1	-3.313910	-1.260015	-0.719425
23	1	-2.965853	-3.012115	-0.493591
24	5	-1.408342	1.848683	-0.132036
25	9	-1.481961	1.617009	1.254526
26	9	-1.883826	3.142646	-0.420294
27	9	-2.207235	0.897123	-0.805155
28	9	-0.074586	1.728359	-0.562414

Table S18. Computed coordinates: **3**·BF_4 rot TS

atom	*Z*	*x*	*y*	*z*
1	1	4.845634	1.583484	-0.577522
2	1	3.482035	1.774858	0.519038
3	1	5.078556	1.322713	1.155467
4	6	4.378290	1.175122	0.331329
5	6	4.046068	-0.270514	0.170975
6	1	4.767441	-1.031652	0.462827
7	6	2.974506	-0.675679	-0.719559
8	1	3.202669	-0.723001	-1.790433
9	6	1.690924	-0.973861	-0.345969
10	6	1.275049	-0.925669	1.027874
11	6	0.720180	-1.320040	-1.343195
12	6	-0.011582	-1.184325	1.367307
13	1	2.008710	-0.669809	1.785679
14	6	-0.573335	-1.579156	-1.010459
15	1	1.031167	-1.363719	-2.382599
16	6	-0.960913	-1.496451	0.354166
17	1	-0.357824	-1.139210	2.393386
18	1	-1.299104	-1.819318	-1.776186
19	8	-2.175828	-1.703160	0.787057
20	6	-3.242838	-1.978691	-0.132033
21	1	-4.130156	-2.077310	0.486436
22	1	-3.353503	-1.145097	-0.824152
23	1	-3.052664	-2.913203	-0.661826
24	5	-1.377545	1.884976	-0.078740
25	9	-1.529308	1.653049	1.301237
26	9	-1.773134	3.201833	-0.383428
27	9	-2.188760	0.975598	-0.794257
28	9	-0.031765	1.700327	-0.445274

Table S19. Computed coordinates: cycloadduct **5**

atom	*Z*	*x*	*y*	*z*
1	1	-1.692273	3.145448	0.627916
2	1	-0.088431	2.408868	0.497405
3	1	-1.097575	2.587304	-0.940734
4	6	-1.117141	2.357238	0.131038
5	6	-1.739101	0.988412	0.376230
6	1	-1.679055	0.759227	1.450909
7	6	-1.010473	-0.134087	-0.383758
8	1	-1.187861	0.043255	-1.454950
9	6	0.480629	-0.140740	-0.159718
10	6	1.024027	-0.283499	1.124082
11	6	1.369471	-0.004441	-1.220847
12	6	2.393326	-0.289279	1.333220
13	1	0.364889	-0.384581	1.982848
14	6	2.753537	-0.010258	-1.034348
15	1	0.981119	0.112213	-2.230215
16	6	3.271982	-0.153681	0.252719
17	1	2.805201	-0.397358	2.332714
18	1	3.404993	0.098626	-1.894349
19	8	4.596551	-0.172904	0.561337
20	6	5.526916	-0.032098	-0.496013
21	1	6.512873	-0.071251	-0.036495
22	1	5.433578	-0.847403	-1.220797
23	1	5.404872	0.927499	-1.008773
24	6	-1.627079	-1.493926	-0.028457
25	1	-1.273152	-1.812650	0.963286
26	1	-1.249303	-2.256041	-0.722317
27	6	-3.126442	-1.478445	-0.050155
28	1	-3.629594	-2.445874	-0.064854
29	6	-3.860026	-0.361785	-0.055990
30	6	-3.216643	0.997163	-0.019206
31	1	-3.775037	1.646135	0.669549
32	1	-3.329450	1.472119	-1.007167
33	6	-5.357296	-0.377353	-0.111353
34	1	-5.724510	0.191684	-0.974588
35	1	-5.757017	-1.392367	-0.181296
36	1	-5.790803	0.099053	0.776541

Table S20. Computed coordinates: **3**·BF_4·O_2 (superoxo)

atom	*Z*	*x*	*y*	*z*
1	1	3.889395	1.758737	-1.618469
2	1	2.130421	1.547297	-1.482694
3	1	3.045653	2.186459	-0.109794
4	6	3.076384	1.482601	-0.943918
5	6	3.286091	0.059348	-0.447130
6	1	3.367021	-0.646331	-1.277528
7	6	2.232479	-0.321472	0.530066
8	1	2.452629	-0.080055	1.568606
9	6	1.005025	-0.826070	0.226084
10	6	0.602826	-1.183006	-1.109221
11	6	0.037521	-0.946366	1.282430
12	6	-0.666286	-1.581064	-1.360347
13	1	1.314464	-1.132005	-1.925356
14	6	-1.241049	-1.332299	1.034676
15	1	0.337515	-0.692400	2.293830
16	6	-1.619733	-1.628893	-0.301924
17	1	-0.998398	-1.846465	-2.357643
18	1	-1.964195	-1.378846	1.838147
19	8	-2.821616	-1.976921	-0.665191
20	6	-3.897253	-1.985173	0.286281
21	1	-4.779987	-2.252150	-0.286909
22	1	-3.712470	-2.733343	1.058203
23	1	-4.009414	-0.990295	0.715854
24	5	-1.723525	1.959348	0.094208
25	9	-2.659652	0.980870	-0.312635
26	9	-0.478124	1.694920	-0.507453
27	9	-1.587748	1.920306	1.494408
28	9	-2.179160	3.230595	-0.302211
29	8	4.590422	0.038037	0.213134
30	8	4.830084	-1.111517	0.774774

Table S21. Computed coordinates: **3**·BF_4·O_2 (dioxetane)

atom	*Z*	*x*	*y*	*z*
1	1	5.387325	-0.601143	-1.622371
2	1	3.825001	-0.617239	-2.445650
3	1	4.495983	0.920703	-1.856501
4	6	4.393922	-0.144745	-1.639370
5	6	3.694638	-0.368993	-0.333027
6	1	3.585589	-1.431321	-0.093000
7	6	2.413945	0.426252	-0.017200
8	1	2.295330	1.297648	-0.673801
9	6	1.143307	-0.320957	0.100730
10	6	0.737029	-0.878730	1.332099
11	6	0.349472	-0.489718	-1.062096
12	6	-0.444934	-1.555699	1.411166
13	1	1.364052	-0.749945	2.206445
14	6	-0.832505	-1.166054	-1.008758
15	1	0.678188	-0.052064	-1.999040
16	6	-1.262760	-1.691724	0.246084
17	1	-0.803511	-1.987537	2.338822
18	1	-1.448960	-1.269526	-1.891939
19	8	-2.383373	-2.322042	0.438948
20	6	-3.351896	-2.455701	-0.616473
21	1	-4.195544	-2.964354	-0.161122
22	1	-3.639348	-1.463782	-0.962364
23	1	-2.938268	-3.058614	-1.425232
24	5	-2.172018	1.796085	-0.040690
25	9	-2.955456	2.874618	0.404248
26	9	-1.992925	1.877871	-1.433226
27	9	-2.830010	0.581173	0.272448
28	9	-0.919064	1.822647	0.600823
29	8	4.310981	0.315397	0.794052
30	8	3.008647	0.814945	1.230955

Table S22. Computed coordinates: (**3**·BF_4)$_2$

atom	*Z*	*x*	*y*	*z*
1	1	0.194445	-2.190523	2.281657
2	1	-1.398609	-2.443230	1.552318
3	1	0.025416	-2.244967	0.520852
4	6	-0.452010	-1.910079	1.445899
5	6	-0.677238	-0.389940	1.453385
6	1	-1.165881	-0.113174	2.390698
7	6	-1.530307	-0.028942	0.298106
8	1	-1.125620	-0.267943	-0.685275
9	6	-2.778644	0.528036	0.319575
10	6	-3.469740	0.883246	1.528919
11	6	-3.440814	0.767646	-0.932070
12	6	-4.713870	1.418960	1.479201
13	1	-2.999281	0.717568	2.490676
14	6	-4.686794	1.308948	-0.990369
15	1	-2.929111	0.497411	-1.850228
16	6	-5.352167	1.623469	0.222611
17	1	-5.259494	1.685942	2.377362
18	1	-5.173277	1.460520	-1.944604
19	8	-6.558035	2.118177	0.295190
20	6	-7.336534	2.315940	-0.894697
21	1	-8.293664	2.693395	-0.547048
22	1	-6.857277	3.053232	-1.540106
23	1	-7.466015	1.363679	-1.407230
24	5	-5.890278	-1.857061	-0.722235
25	9	-6.803645	-0.809883	-0.464636
26	9	-4.861852	-1.825007	0.237692
27	9	-5.343041	-1.694247	-2.008952
28	9	-6.564827	-3.091128	-0.650144
29	1	-0.194626	2.189266	2.282149
30	1	1.398575	2.442221	1.553225
31	1	-0.025223	2.244231	0.521398
32	6	0.452013	1.909080	1.446447
33	6	1.530362	0.028274	0.298166
34	1	1.125619	0.267369	-0.685167
35	6	2.778806	-0.528474	0.319518
36	6	3.469981	-0.883783	1.528789
37	6	3.441024	-0.767679	-0.932175
38	6	4.714240	-1.419185	1.478959
39	1	2.999459	-0.718459	2.490576
40	6	4.687128	-1.308693	-0.990585
41	1	2.929272	-0.497363	-1.850283
42	6	5.352578	-1.623293	0.222326
43	1	5.259924	-1.686237	2.377064
44	1	5.173633	-1.459959	-1.944857
45	8	6.558570	-2.117726	0.294804
46	6	7.337037	-2.315220	-0.895144
47	1	8.294262	-2.692522	-0.547592
48	1	6.857882	-3.052543	-1.540595
49	1	7.466310	-1.362895	-1.407611
50	5	5.889763	1.857442	-0.721988
51	9	6.803730	0.810745	-0.464526
52	9	4.861531	1.824873	0.238136
53	9	5.342406	1.694345	-2.008596
54	9	6.563688	3.091867	-0.650009
55	6	0.677251	0.388934	1.453524
56	1	1.165860	0.111906	2.390770

Table S23. Computed coordinates: (**3**·BF_4)$_2$·O_2

atom	*Z*	*x*	*y*	*z*
1	1	0.927061	2.894937	-0.326630
2	1	2.612894	2.422112	-0.005739
3	1	2.034500	2.544506	-1.675364
4	6	1.753687	2.263100	-0.658537
5	6	1.326156	0.798305	-0.600583
6	1	1.021206	0.537980	0.418295
7	6	2.437689	-0.060945	-1.086217
8	1	2.490000	-0.169247	-2.168488
9	6	3.420506	-0.621851	-0.325431
10	6	3.447987	-0.543022	1.110450
11	6	4.525146	-1.251452	-0.992022
12	6	4.515431	-1.006924	1.803730
13	1	2.614775	-0.103648	1.646603
14	6	5.606515	-1.704434	-0.303532
15	1	4.501838	-1.331860	-2.073939
16	6	5.630036	-1.555620	1.107967
17	1	4.567962	-0.947500	2.885003
18	1	6.447637	-2.137889	-0.828414
19	8	6.630307	-1.908814	1.868255
20	6	7.851853	-2.386589	1.285479
21	1	8.522429	-2.547382	2.124355
22	1	7.678622	-3.327086	0.760947
23	1	8.256820	-1.628430	0.615589
24	5	6.545699	1.674483	-0.309689
25	9	7.169308	0.766823	0.575590
26	9	5.198393	1.842937	0.063114
27	9	6.612463	1.169516	-1.621633
28	9	7.210034	2.914517	-0.246409
29	8	0.207028	0.688131	-1.468731
30	8	-0.206871	-0.688835	-1.468989
31	1	-0.926241	-2.895894	-0.327119
32	1	-2.612321	-2.423887	-0.006557
33	1	-2.033485	-2.545746	-1.676073
34	6	-1.753043	-2.264346	-0.659140
35	6	-1.326059	-0.799412	-0.600928
36	1	-1.021272	-0.539088	0.417987
37	6	-2.437761	0.059553	-1.086676
38	1	-2.490318	0.167262	-2.168998
39	6	-3.420359	0.620930	-0.325975
40	6	-3.447497	0.542907	1.109959
41	6	-4.525107	1.250277	-0.992648
42	6	-4.514668	1.007412	1.803250
43	1	-2.614247	0.103642	1.646143
44	6	-5.606201	1.703864	-0.304140
45	1	-4.502092	1.329996	-2.074623
46	6	-5.629318	1.556001	1.107471
47	1	-4.566940	0.948604	2.884570
48	1	-6.447405	2.137127	-0.829049
49	8	-6.629233	1.910022	1.867824
50	6	-7.850795	2.387831	1.285097
51	1	-8.521078	2.549355	2.124067
52	1	-7.677384	3.327949	0.759941
53	1	-8.256210	1.629391	0.615800
54	5	-6.546713	-1.673830	-0.308848
55	9	-7.169592	-0.765326	0.576090
56	9	-5.199326	-1.842571	0.063494
57	9	-6.613834	-1.169684	-1.621099
58	9	-7.211525	-2.913546	-0.244473

Table S24. Computed coordinates: **5**·BF_4

atom	*Z*	*x*	*y*	*z*
1	1	1.761099	2.915113	-0.496442
2	1	0.465146	1.718608	-0.384217
3	1	1.404324	2.142879	1.051372
4	6	1.468398	1.970111	-0.028877
5	6	2.484768	0.878520	-0.341339
6	1	2.479677	0.677738	-1.421718
7	6	2.160414	-0.449554	0.385156
8	1	2.313269	-0.280520	1.458440
9	6	0.753278	-0.879556	0.170533
10	6	0.265318	-1.140866	-1.137626
11	6	-0.131018	-1.015994	1.271632
12	6	-1.035196	-1.490481	-1.337707
13	1	0.929382	-1.040689	-1.989066
14	6	-1.441168	-1.363355	1.101590
15	1	0.246388	-0.824515	2.270859
16	6	-1.919528	-1.596604	-0.220367
17	1	-1.439290	-1.675615	-2.326664
18	1	-2.107190	-1.444154	1.950188
19	8	-3.145099	-1.919377	-0.519981
20	6	-4.156228	-2.040934	0.497652
21	1	-5.070186	-2.266554	-0.042501
22	1	-3.900552	-2.860801	1.169666
23	1	-4.246668	-1.096780	1.031140
24	6	3.145212	-1.546863	-0.069486
25	1	2.893131	-1.884227	-1.084009
26	1	3.024801	-2.428854	0.570296
27	6	4.564649	-1.065995	-0.025072
28	1	5.335816	-1.835950	-0.036069
29	6	4.920138	0.219826	0.036183
30	6	3.892291	1.317475	0.053188
31	1	4.212439	2.126164	-0.617592
32	1	3.870967	1.772079	1.055725
33	6	6.349233	0.660735	0.110989
34	1	6.522017	1.278437	1.000727
35	1	7.040308	-0.185040	0.145979
36	1	6.614718	1.283074	-0.751950
37	5	-3.296296	1.580200	-0.032242
38	9	-3.425981	2.973307	0.088776
39	9	-3.265792	0.994222	1.254009
40	9	-2.100932	1.269095	-0.709237
41	9	-4.388483	1.055025	-0.748191

Table S25. Computed coordinates: **5** (dioxetane)

atom	*Z*	*x*	*y*	*z*
1	1	-1.034072	3.251857	-0.911600
2	1	0.514150	2.417390	-0.715312
3	1	-0.537283	2.018541	-2.077109
4	6	-0.528869	2.286553	-1.014253
5	6	-1.222074	1.213927	-0.183416
6	1	-1.175311	1.505099	0.877230
7	6	-0.550387	-0.164129	-0.337864
8	1	-0.712144	-0.483228	-1.376490
9	6	0.938253	-0.131662	-0.095611
10	6	1.469859	0.290646	1.130017
11	6	1.834518	-0.509121	-1.089693
12	6	2.837034	0.333864	1.347107
13	1	0.805679	0.602602	1.932363
14	6	3.216205	-0.476213	-0.892160
15	1	1.454521	-0.838144	-2.054232
16	6	3.724068	-0.050561	0.335506
17	1	3.241079	0.666577	2.299048
18	1	3.874368	-0.780212	-1.698382
19	8	5.045221	0.027269	0.646190
20	6	5.984068	-0.340784	-0.347571
21	1	6.966232	-0.200984	0.100195
22	1	5.865470	-1.389464	-0.638799
23	1	5.896293	0.296517	-1.233391
24	6	-1.221388	-1.183165	0.590592
25	1	-0.953452	-0.960722	1.631046
26	1	-0.843652	-2.194328	0.396488
27	6	-2.724621	-1.191899	0.517837
28	1	-3.159667	-1.726759	1.371219
29	6	-3.491922	0.091042	0.213873
30	6	-2.688594	1.101868	-0.606332
31	1	-3.174767	2.082544	-0.558434
32	1	-2.717483	0.787678	-1.655900
33	6	-4.291613	0.716522	1.324391
34	1	-5.015446	1.431411	0.921693
35	1	-4.827104	-0.035340	1.908263
36	1	-3.623030	1.266670	1.993842
37	8	-3.283123	-1.753941	-0.701108
38	8	-4.331047	-0.728206	-0.678364

Table S26. Computed coordinates: **5**·BF_4·O_2 (dioxetane)

atom	*Z*	*x*	*y*	*z*
1	1	-1.302166	3.040578	0.465177
2	1	-0.013790	1.838074	0.331915
3	1	-0.979279	2.259068	-1.086065
4	6	-1.022546	2.093097	-0.004029
5	6	-2.035078	1.004544	0.332536
6	1	-2.045421	0.846775	1.420392
7	6	-1.684709	-0.334764	-0.356001
8	1	-1.802871	-0.191472	-1.436444
9	6	-0.284866	-0.772587	-0.090887
10	6	0.187473	-0.927783	1.238976
11	6	0.594554	-1.045528	-1.169049
12	6	1.471351	-1.311647	1.479680
13	1	-0.473953	-0.723965	2.073710
14	6	1.888768	-1.428965	-0.959031
15	1	0.228293	-0.934073	-2.184441
16	6	2.352872	-1.559975	0.382652
17	1	1.863490	-1.423612	2.484317
18	1	2.553340	-1.613905	-1.792392
19	8	3.559757	-1.910249	0.720054
20	6	4.571976	-2.164245	-0.271853
21	1	5.470401	-2.383323	0.296231
22	1	4.283912	-3.026412	-0.874089
23	1	4.707913	-1.273417	-0.881882
24	6	-2.658105	-1.439974	0.101189
25	1	-2.465964	-1.695825	1.149456
26	1	-2.496958	-2.359997	-0.471074
27	6	-4.104895	-1.035225	-0.000557
28	1	-4.736176	-1.728957	0.567993
29	6	-4.528408	0.414482	0.212061
30	6	-3.430536	1.425454	-0.125889
31	1	-3.682418	2.399716	0.305995
32	1	-3.409931	1.558538	-1.212987
33	6	-5.296856	0.752746	1.460065
34	1	-5.792514	1.722150	1.353609
35	1	-6.049831	-0.005085	1.686501
36	1	-4.608401	0.825559	2.307612
37	5	3.816677	1.514743	-0.125026
38	9	4.771892	0.964764	0.750198
39	9	4.093656	2.873219	-0.345644
40	9	2.532701	1.374055	0.437087
41	9	3.863368	0.814735	-1.353014
42	8	-4.624118	-0.939973	-1.350464
43	8	-5.412086	0.229863	-0.951497

Table S27. Computed coordinates: **5**·BF_4·O_2 (superoxo)

atom	*Z*	*x*	*y*	*z*
1	1	0.795288	2.967558	-0.602760
2	1	-0.338972	1.654742	-0.270885
3	1	0.794312	2.179258	0.980780
4	6	0.678622	2.005828	-0.094766
5	6	1.702809	0.996085	-0.592008
6	1	1.546068	0.828597	-1.665779
7	6	1.596323	-0.355965	0.130743
8	1	1.739698	-0.172159	1.203767
9	6	0.235931	-0.984630	-0.044982
10	6	-0.228627	-1.384665	-1.303597
11	6	-0.609374	-1.156976	1.045563
12	6	-1.491967	-1.928886	-1.461575
13	1	0.396237	-1.263450	-2.184939
14	6	-1.884913	-1.702003	0.907462
15	1	-0.277498	-0.851441	2.034802
16	6	-2.335830	-2.084020	-0.356622
17	1	-1.851341	-2.228282	-2.441746
18	1	-2.514087	-1.805521	1.783909
19	8	-3.561109	-2.604101	-0.617988
20	6	-4.488982	-2.687629	0.450587
21	1	-5.405242	-3.087613	0.020176
22	1	-4.133966	-3.364513	1.234315
23	1	-4.686394	-1.698859	0.874550
24	6	2.705672	-1.301105	-0.343099
25	1	2.598849	-1.516785	-1.412007
26	1	2.656787	-2.264046	0.173204
27	6	4.086437	-0.726165	-0.145356
28	1	4.888039	-1.356291	-0.530182
29	6	4.243977	0.700235	-0.554704
30	6	3.112222	1.586449	-0.444950
31	1	3.271174	2.511163	-1.008113
32	1	3.251950	1.912971	0.617616
33	6	5.563294	1.152616	-0.921312
34	1	5.675911	2.233284	-0.976427
35	1	6.331646	0.668256	-0.303180
36	1	5.741750	0.722344	-1.926542
37	5	-3.618746	2.005865	0.187276
38	9	-4.231213	3.261097	-0.012386
39	9	-2.916005	2.019442	1.408065
40	9	-2.726246	1.749157	-0.871430
41	9	-4.608765	1.003447	0.224271
42	8	4.324187	-0.626302	1.340590
43	8	5.566923	-0.666078	1.664657

Table S28. Computed coordinates: **5**·BF_4·O_2 (superoxo TS)

atom	*Z*	*x*	*y*	*z*
1	1	0.792092	2.953061	-0.685806
2	1	-0.342957	1.624870	-0.418618
3	1	0.739313	2.134073	0.880737
4	6	0.665303	1.980014	-0.201650
5	6	1.722663	0.993787	-0.677537
6	1	1.591596	0.824616	-1.755052
7	6	1.619216	-0.366142	0.034058
8	1	1.806430	-0.193287	1.102767
9	6	0.251743	-0.988212	-0.095663
10	6	-0.260253	-1.373162	-1.340572
11	6	-0.556018	-1.165032	1.022263
12	6	-1.531857	-1.907838	-1.458930
13	1	0.333057	-1.243566	-2.242553
14	6	-1.839733	-1.699915	0.924416
15	1	-0.187283	-0.870520	2.001846
16	6	-2.337249	-2.068171	-0.326066
17	1	-1.927991	-2.195370	-2.428431
18	1	-2.438198	-1.807340	1.821695
19	8	-3.574087	-2.579408	-0.548360
20	6	-4.464154	-2.666018	0.551544
21	1	-5.397839	-3.056202	0.150556
22	1	-4.086618	-3.352143	1.316558
23	1	-4.639806	-1.679713	0.990462
24	6	2.704669	-1.314731	-0.486875
25	1	2.511522	-1.592563	-1.533597
26	1	2.712675	-2.263808	0.060059
27	6	4.063012	-0.725029	-0.466431
28	1	4.897329	-1.362559	-0.750230
29	6	4.257757	0.687563	-0.584016
30	6	3.114281	1.596998	-0.470664
31	1	3.288514	2.471170	-1.110461
32	1	3.196665	2.021147	0.551278
33	6	5.622743	1.181091	-0.650448
34	1	5.703551	2.263842	-0.717081
35	1	6.142993	0.831412	0.269968
36	1	6.185061	0.689690	-1.452736
37	5	-3.655719	1.990942	0.200983
38	9	-4.280508	3.244193	0.028652
39	9	-2.918832	1.999080	1.401685
40	9	-2.792050	1.747578	-0.884370
41	9	-4.638843	0.982644	0.258030
42	8	4.411964	-0.778090	1.388806
43	8	5.521855	-0.505524	1.792952

Table S29. Computed coordinates: isoprene, **4**

atom	*Z*	*x*	*y*	*z*
1	6	-1.976933	0.001898	0.000108
2	1	-2.007921	1.087894	0.000307
3	1	-2.935244	-0.508635	0.000025
4	6	-0.827185	-0.683024	-0.000109
5	1	-0.865996	-1.772555	-0.000376
6	6	0.514544	-0.097233	-0.000030
7	6	1.588022	-0.902602	0.000084
8	1	2.600118	-0.507904	0.000233
9	1	1.486175	-1.984938	0.000069
10	6	0.649746	1.397986	-0.000056
11	1	0.167965	1.840319	-0.878704
12	1	0.167942	1.840493	0.878493
13	1	1.697799	1.703179	-0.000024

Table S30. Computed coordinates: **4**·BF_4

atom	*Z*	*x*	*y*	*z*
1	6	-2.407102	1.720801	-0.070172
2	1	-2.784093	1.537098	-1.070356
3	1	-2.521405	2.724366	0.323828
4	6	-1.800367	0.742448	0.671751
5	1	-1.433690	0.990377	1.662976
6	6	-1.602874	-0.582306	0.212485
7	6	-0.946871	-1.451118	1.084980
8	1	-0.791039	-2.492260	0.830744
9	1	-0.601967	-1.113518	2.055381
10	6	-2.018257	-1.046732	-1.138447
11	1	-3.054875	-0.783740	-1.361807
12	1	-1.386336	-0.565228	-1.891863
13	1	-1.904179	-2.125205	-1.241060
14	5	1.645427	0.147216	-0.097791
15	9	1.310234	0.875805	1.057012
16	9	1.377480	-1.230317	0.140360
17	9	3.003379	0.307703	-0.396905
18	9	0.853715	0.579417	-1.176298

Table S31. Computed coordinates: **3·4**

atom	*Z*	*x*	*y*	*z*
1	6	2.446528	1.979355	-0.253886
2	1	2.883594	1.404291	-1.065013
3	1	3.126567	2.326404	0.519358
4	6	1.129320	2.228878	-0.201623
5	6	0.253896	1.730800	-1.261598
6	6	0.519441	3.005569	0.928139
7	1	0.027579	3.915959	0.567650
8	1	-0.246734	2.413752	1.439068
9	1	1.272100	3.297609	1.663428
10	6	-1.068250	1.919536	-1.328978
11	1	-1.656350	1.500516	-2.139395
12	1	0.742393	1.146437	-2.040733
13	1	-1.615412	2.477762	-0.574816
14	1	5.017418	-0.687311	-0.234620
15	1	4.967248	-2.060782	0.854585
16	1	4.483897	-2.265823	-0.837431
17	6	4.440835	-1.585750	0.017866
18	6	3.036050	-1.237874	0.383287
19	1	2.916696	-0.553010	1.222007
20	6	1.951288	-1.687916	-0.258901
21	1	2.099985	-2.351535	-1.112850
22	6	0.557407	-1.355138	0.032211
23	6	0.155094	-0.638394	1.172454
24	6	-0.441390	-1.746176	-0.863044
25	6	-1.169098	-0.310532	1.384388
26	1	0.893087	-0.324894	1.904432
27	6	-1.780602	-1.419216	-0.669226
28	1	-0.166115	-2.310541	-1.751360
29	6	-2.148872	-0.680412	0.455353
30	1	-1.470992	0.248628	2.265476
31	1	-2.514966	-1.730929	-1.403384
32	8	-3.414805	-0.280222	0.742362
33	6	-4.433339	-0.580025	-0.193867
34	1	-5.348012	-0.147031	0.207013
35	1	-4.217815	-0.133151	-1.169800
36	1	-4.565574	-1.660809	-0.307965

Table S32. Computed coordinates: **3·4**·BF_4

atom	*Z*	*x*	*y*	*z*
1	6	-1.302437	1.036367	-2.209461
2	1	-1.203631	-0.035995	-2.350293
3	1	-2.287252	1.464149	-2.370260
4	6	-0.251972	1.793683	-1.841836
5	6	1.037523	1.157661	-1.614952
6	6	-0.388699	3.269069	-1.619655
7	1	-0.119134	3.536552	-0.591790
8	1	0.281217	3.835528	-2.275097
9	1	-1.409782	3.608339	-1.801595
10	6	2.147429	1.792100	-1.204470
11	1	3.064825	1.240476	-1.029195
12	1	1.076543	0.079014	-1.756038
13	1	2.176025	2.866059	-1.044501
14	1	2.553229	2.405316	3.140988
15	1	3.038468	2.769258	1.503870
16	1	1.674380	3.655710	2.236021
17	6	2.161362	2.682658	2.152606
18	6	1.251362	1.621087	1.672732
19	1	1.698714	0.654837	1.457117
20	6	-0.106359	1.783880	1.559758
21	1	-0.525306	2.756599	1.812440
22	6	-1.022876	0.790679	1.130531
23	6	-0.631410	-0.537366	0.789623
24	6	-2.402985	1.124196	1.045042
25	6	-1.561918	-1.458577	0.408057
26	1	0.410871	-0.828301	0.825527
27	6	-3.346499	0.205672	0.661014
28	1	-2.713324	2.134664	1.293223
29	6	-2.931924	-1.104862	0.333941
30	1	-1.275605	-2.470356	0.141432
31	1	-4.389504	0.492093	0.604905
32	8	-3.741985	-2.073761	-0.058618
33	6	-5.145324	-1.827629	-0.178216
34	1	-5.575141	-2.767334	-0.513534
35	1	-5.568751	-1.549871	0.788766
36	1	-5.335220	-1.047762	-0.917933
37	5	2.914548	-1.958633	-0.132296
38	9	1.726184	-2.135422	-0.867785
39	9	3.792809	-1.122091	-0.842733
40	9	3.521238	-3.205241	0.095357
41	9	2.599755	-1.358073	1.111614

Table S33. Computed coordinates: **3·4**·BF_4 (ts)

atom	*Z*	*x*	*y*	*z*
1	6	1.345816	0.369969	2.415959
2	1	0.978653	-0.646327	2.518724
3	1	2.372515	0.556465	2.714449
4	6	0.554602	1.358866	1.920620
5	6	-0.786569	1.032041	1.540082
6	6	1.055816	2.765555	1.777352
7	1	0.922755	3.136587	0.757210
8	1	0.505106	3.446222	2.434800
9	1	2.115795	2.837325	2.024757
10	6	-1.656565	1.907820	0.933424
11	1	-2.688943	1.609148	0.797706
12	1	-1.110052	0.003118	1.677541
13	1	-1.440883	2.969482	0.879207
14	1	-2.578651	2.492488	-2.857941
15	1	-3.327691	2.632206	-1.277005
16	1	-1.952845	3.676810	-1.704208
17	6	-2.367893	2.670753	-1.795591
18	6	-1.423573	1.620404	-1.314482
19	1	-1.828593	0.618293	-1.211166
20	6	-0.048713	1.777241	-1.435708
21	1	0.319523	2.770150	-1.691991
22	6	0.926663	0.785278	-1.167245
23	6	0.597491	-0.565275	-0.877910
24	6	2.290051	1.157932	-1.128588
25	6	1.575110	-1.469947	-0.555203
26	1	-0.433262	-0.898061	-0.913631
27	6	3.278724	0.258953	-0.792365
28	1	2.563227	2.185447	-1.352298
29	6	2.923937	-1.068633	-0.490417
30	1	1.330841	-2.502669	-0.328394
31	1	4.311217	0.584826	-0.757226
32	8	3.788130	-2.022794	-0.138305
33	6	5.173793	-1.706115	-0.041222
34	1	5.663547	-2.627465	0.263809
35	1	5.567870	-1.383857	-1.008005
36	1	5.343954	-0.933219	0.712194
37	5	-3.116695	-1.705441	0.138022
38	9	-2.052877	-2.039470	0.999064
39	9	-3.722704	-0.513734	0.582283
40	9	-4.060516	-2.742564	0.118806
41	9	-2.606991	-1.502727	-1.166201

Table S34. Computed coordinates: **5·4**

atom	*Z*	*x*	*y*	*z*
1	1	-3.416327	-3.255022	0.124975
2	1	-1.680595	-2.919474	0.039634
3	1	-2.584144	-2.526780	1.504603
4	6	-2.636836	-2.540456	0.409517
5	6	-2.944860	-1.150165	-0.132171
6	1	-2.916693	-1.184576	-1.231936
7	6	-1.920098	-0.096827	0.328160
8	1	-2.053898	0.017484	1.414297
9	6	-0.492886	-0.517507	0.083067
10	6	-0.020200	-0.777658	-1.209277
11	6	0.393865	-0.699296	1.138563
12	6	1.280388	-1.195574	-1.432131
13	1	-0.682647	-0.656309	-2.063015
14	6	1.707330	-1.124253	0.937788
15	1	0.057413	-0.511131	2.155940
16	6	2.158364	-1.370965	-0.357716
17	1	1.639601	-1.391261	-2.438702
18	1	2.360010	-1.253880	1.793582
19	8	3.411734	-1.789474	-0.676977
20	6	4.321001	-2.009572	0.384051
21	1	5.255119	-2.323735	-0.078784
22	1	4.492479	-1.092085	0.953656
23	1	3.964743	-2.800133	1.053314
24	6	-2.232715	1.257035	-0.322394
25	1	-1.880779	1.258506	-1.364542
26	1	-1.648198	2.040717	0.174892
27	6	-3.690842	1.604964	-0.278845
28	1	-3.955973	2.641521	-0.490528
29	6	-4.659202	0.730313	0.008189
30	6	-4.348682	-0.714826	0.287825
31	1	-5.093713	-1.349942	-0.211096
32	1	-4.487055	-0.909601	1.363513
33	6	-6.104669	1.117710	0.082467
34	1	-6.527738	0.866424	1.063065
35	1	-6.254476	2.187349	-0.086279
36	1	-6.700255	0.569566	-0.657866
37	6	1.300056	2.419628	-0.340374
38	1	1.087592	2.619500	0.705749
39	1	0.482043	2.571075	-1.036478
40	6	2.492680	1.987220	-0.760731
41	1	2.634315	1.790874	-1.823344
42	6	3.657017	1.737894	0.087854
43	6	4.809478	1.335048	-0.467746
44	1	5.696639	1.140134	0.128236

Table S34 continued

atom	*Z*	*x*	*y*	*z*
45	1	4.897834	1.177878	-1.539653
46	6	3.525841	1.942727	1.568630
47	1	3.280394	2.983722	1.806875
48	1	2.719723	1.325401	1.977167
49	1	4.450516	1.686930	2.090201

Table S35. Computed coordinates: **5**·**4**·BF_4

atom	*Z*	*x*	*y*	*z*
1	1	-1.723842	-3.387301	0.631388
2	1	-0.449076	-2.214259	0.293479
3	1	-1.423331	-2.066678	1.763267
4	6	-1.457038	-2.327949	0.699353
5	6	-2.484766	-1.476940	-0.036760
6	1	-2.421861	-1.692131	-1.113407
7	6	-2.255160	0.054054	0.130661
8	1	-2.468195	0.293399	1.181225
9	6	-0.824737	0.384949	-0.139807
10	6	-0.302321	0.402976	-1.456339
11	6	0.080629	0.522715	0.941340
12	6	1.042032	0.497735	-1.676018
13	1	-0.971928	0.308630	-2.303828
14	6	1.433798	0.603301	0.749314
15	1	-0.313363	0.530929	1.952524
16	6	1.940381	0.567889	-0.575166
17	1	1.460547	0.487189	-2.676507
18	1	2.105070	0.664446	1.595466
19	8	3.212794	0.577735	-0.895490
20	6	4.209850	0.672315	0.126649
21	1	5.161092	0.646331	-0.396908
22	1	4.101625	1.619865	0.659437
23	1	4.126966	-0.173564	0.807599
24	6	-3.255507	0.813806	-0.749517
25	1	-2.958574	0.766057	-1.805666
26	1	-3.231282	1.876854	-0.491251
27	6	-4.654815	0.296011	-0.597876
28	1	-5.452840	0.945593	-0.957088
29	6	-4.964124	-0.881530	-0.050211
30	6	-3.894951	-1.815324	0.441610
31	1	-4.136434	-2.840902	0.130571
32	1	-3.914087	-1.840450	1.542365
33	6	-6.376204	-1.349322	0.122411
34	1	-6.587168	-1.578630	1.174150
35	1	-7.101140	-0.603583	-0.213439
36	1	-6.556062	-2.275732	-0.436250
37	5	2.807413	-2.847360	0.118065
38	9	2.553831	-4.190577	0.452183
39	9	2.782871	-2.059257	1.289487
40	9	1.821725	-2.388547	-0.775318
41	9	4.075738	-2.738156	-0.484586
42	6	2.493273	3.753172	-0.170037
43	1	2.798023	3.905870	0.860915
44	1	3.284035	3.707421	-0.911775
45	6	1.199757	3.644749	-0.525947
46	1	0.953884	3.516039	-1.578515
47	6	0.079839	3.682796	0.396033
48	6	-1.169388	3.548148	-0.094621
49	1	-2.037666	3.578291	0.556058
50	1	-1.351880	3.441002	-1.159690
51	6	0.332737	3.854232	1.862595
52	1	0.994227	3.071017	2.246134
53	1	0.823530	4.811134	2.068927
54	1	-0.596879	3.820204	2.432511
atom	*Z*	*x*	*y*	*z*

Table S36. Computed coordinates: $[Cr(bpy)_3](BF_4)_3$ ααα

atom	*Z*	*x*	*y*	*z*
1	5	-4.714643	-1.349364	-1.210981
2	9	-4.055299	-0.563149	-2.180883
3	9	-3.754159	-1.949129	-0.370553
4	9	-5.560306	-0.527375	-0.442264
5	9	-5.470324	-2.347428	-1.849318
6	5	0.812126	4.611301	-0.971533
7	9	0.180608	5.803002	-1.369386
8	9	2.074878	4.901571	-0.419472
9	9	0.019175	3.957612	-0.006594
10	9	0.974991	3.768380	-2.091275
11	24	-0.076650	-0.150777	0.432054
12	7	1.149414	-1.505341	1.319628
13	6	1.146492	-2.724662	0.740230
14	6	1.928102	-3.753710	1.243152
15	6	2.724564	-3.517569	2.353993
16	6	2.726517	-2.257394	2.935331
17	6	1.924577	-1.275032	2.382010
18	1	1.926357	-4.727829	0.772205
19	1	3.342961	-4.312798	2.755990
20	1	3.336945	-2.028762	3.800806
21	1	1.888758	-0.280137	2.803610
22	7	-1.685050	-0.610083	1.581410
23	7	0.540524	1.377151	1.615492
24	7	-0.426497	-1.748533	-0.751215
25	7	1.475181	0.529446	-0.672929
26	7	-1.463177	1.051993	-0.416441
27	6	0.264134	-2.861399	-0.421067
28	6	-2.775912	0.149590	1.346307
29	6	-1.714432	-1.546771	2.533465
30	6	1.682634	1.968661	1.206475
31	6	-0.053908	1.777600	2.742956
32	6	-1.261554	-1.756518	-1.792452
33	6	2.202356	1.499967	-0.079588
34	6	1.835688	0.062131	-1.868794
35	6	-2.649486	1.089227	0.230529
36	6	-1.253823	1.831310	-1.477244
37	6	0.123791	-4.026479	-1.159033
38	6	-3.922471	0.006798	2.114902
39	6	-2.832555	-1.756512	3.321448
40	1	-0.813552	-2.129977	2.667875
41	6	2.281270	2.962122	1.968861
42	6	0.477565	2.777113	3.538404
43	1	-0.968963	1.269825	3.016049
44	6	-1.439849	-2.884494	-2.575896
45	1	-1.802831	-0.844203	-1.992910
46	6	3.331047	2.019462	-0.692586
47	6	2.940115	0.551363	-2.544976
48	1	1.224554	-0.723568	-2.288884
49	6	-3.657658	1.944086	-0.183047
50	6	-2.228056	2.692196	-1.956661
51	1	-0.280619	1.774710	-1.941263
52	6	-0.735115	-4.035063	-2.251173
53	1	0.681981	-4.915916	-0.897540
54	6	-3.948853	-0.954957	3.113787
55	1	-4.792127	0.619833	1.922745
56	1	-2.817420	-2.527320	4.082808
57	6	1.673398	3.367830	3.147272
58	1	3.198452	3.429744	1.638888
59	1	-0.035618	3.072908	4.445601
60	1	-2.126987	-2.851493	-3.412694
61	6	3.700813	1.540705	-1.941712
62	1	3.902364	2.805796	-0.218471
63	1	3.197359	0.145675	-3.515436
64	6	-3.442881	2.753492	-1.292267
65	1	-4.607637	1.965593	0.333320
66	1	-2.016484	3.308033	-2.822244
67	1	-0.850530	-4.938299	-2.841003
68	1	-4.839503	-1.083339	3.719743
69	1	2.127083	4.146113	3.751679
70	1	4.577258	1.943227	-2.438418
71	1	-4.225693	3.423221	-1.632445
72	5	4.174124	-2.294192	-0.960525
73	9	5.103300	-1.775019	-1.881106
74	9	2.994186	-2.665012	-1.642434
75	9	4.720651	-3.427773	-0.328352
76	9	3.866038	-1.318135	0.004804

Table S37. Computed coordinates: $[Cr(bpy)_3](BF_4)_2$ βααα

atom	*Z*	*x*	*y*	*z*
1	5	-4.282188	-2.045902	-0.972773
2	9	-3.668962	-1.423936	-2.081204
3	9	-3.316649	-2.294896	0.019606
4	9	-5.285849	-1.204050	-0.457838
5	9	-4.857075	-3.266254	-1.384046
6	24	-0.021188	0.393629	0.245258
7	7	1.463725	-0.292040	1.456960
8	6	1.785003	-1.591491	1.298650
9	6	2.772549	-2.183933	2.073148
10	6	3.432078	-1.419604	3.024917
11	6	3.098632	-0.079699	3.172973
12	6	2.110296	0.447524	2.358249
13	1	3.032582	-3.225479	1.935382
14	1	4.205939	-1.867775	3.639214
15	1	3.594948	0.553419	3.899279
16	1	1.814262	1.486925	2.421847
17	7	-1.532755	-0.079707	1.496150
18	7	0.048573	2.297858	0.827671
19	7	0.091530	-1.545172	-0.366826
20	7	1.309848	1.107758	-1.069782
21	7	-1.591828	0.951518	-0.869389
22	6	1.008392	-2.299739	0.273445
23	6	-2.739166	0.411882	1.126002
24	6	-1.417928	-0.760391	2.644509
25	6	0.712376	3.134763	-0.022098
26	6	-0.620243	2.826750	1.872628
27	6	-0.679001	-2.082016	-1.313175
28	6	1.443282	2.460824	-1.072085
29	6	1.983552	0.373659	-1.969109
30	6	-2.762862	1.034347	-0.185874
31	6	-1.534634	1.422791	-2.125751
32	6	1.173935	-3.640616	-0.042946
33	6	-3.854388	0.262754	1.948576
34	6	-2.487504	-0.961060	3.493640
35	1	-0.431043	-1.136480	2.882925
36	6	0.680179	4.517596	0.162162
37	6	-0.672610	4.181968	2.111946
38	1	-1.116031	2.121615	2.527129
39	6	-0.559492	-3.411908	-1.686492
40	1	-1.413027	-1.429865	-1.764893
41	6	2.254744	3.094855	-2.016300
42	6	2.795971	0.941681	-2.926201
43	1	1.862603	-0.697914	-1.900691
44	6	-3.882161	1.640968	-0.747389
45	6	-2.616834	2.013986	-2.745694
46	1	-0.585074	1.314549	-2.634047
47	6	0.382732	-4.199800	-1.039038
48	1	1.912663	-4.243213	0.469731
49	6	-3.727895	-0.424428	3.141420
50	1	-4.814675	0.655884	1.641795
51	1	-2.349842	-1.517771	4.413434
52	6	-0.016819	5.050972	1.230554
53	1	1.200799	5.169374	-0.529570
54	1	-1.221875	4.554065	2.969453
55	1	-1.202824	-3.813366	-2.460650
56	6	2.929260	2.333489	-2.951977
57	1	2.357685	4.173361	-2.011788
58	1	3.322785	0.307683	-3.629005
59	6	-3.811479	2.141768	-2.035649
60	1	-4.804459	1.708530	-0.184595
61	1	-2.520397	2.375298	-3.763366
62	1	0.502754	-5.245750	-1.302190
63	1	-4.588363	-0.554631	3.789584
64	1	-0.050424	6.124459	1.382907
65	1	3.561455	2.813811	-3.691676
66	1	-4.676101	2.617093	-2.486793
67	5	4.800632	-1.124865	-0.587416
68	9	5.551830	-0.712711	-1.706869
69	9	3.774936	-1.997871	-1.010048
70	9	5.643442	-1.802785	0.316929
71	9	4.238161	-0.002598	0.043427

Table S38. Computed coordinates: $[Cr(Ph_2phen)_3](BF_4)_3$, **2** ααα

atom	*Z*	*x*	*y*	*z*
1	24	0.000481	0.001172	-0.003969
2	7	-0.455193	1.630900	1.097635
3	6	0.156568	2.747624	0.641310
4	6	0.015813	3.999642	1.256916
5	6	-0.831922	4.077834	2.393149
6	6	-1.429044	2.911577	2.840559
7	6	-1.229343	1.711087	2.166935
8	6	0.747536	5.099392	0.714262
9	1	-2.088169	2.929344	3.700481
10	1	-1.705632	0.797830	2.497526
11	7	1.637233	-0.415876	1.102884
12	7	-1.182445	-1.206198	1.100776
13	7	1.005691	1.369574	-1.079302
14	7	-1.686996	0.183892	-1.079876
15	7	0.687385	-1.554523	-1.075072
16	6	0.975157	2.597173	-0.513342
17	6	2.303250	-1.501510	0.647528
18	6	2.088669	0.214896	2.174053
19	6	-2.454432	-1.239926	0.641910
20	6	-0.864987	-1.912252	2.173081
21	6	1.709906	1.181122	-2.181957
22	6	-2.733649	-0.459001	-0.514900
23	6	-1.877279	0.888882	-2.181818
24	6	1.767322	-2.137459	-0.507755
25	6	0.173838	-2.074027	-2.176849
26	6	1.691240	3.685808	-1.025419
27	6	3.458316	-2.002033	1.265432
28	6	3.227019	-0.209995	2.851074
29	1	1.532335	1.081955	2.503975
30	6	-3.467623	-1.988233	1.258269
31	6	-1.804494	-2.684361	2.848455
32	1	0.163218	-1.864010	2.505859
33	6	2.448403	2.207086	-2.763593
34	1	1.710428	0.184906	-2.599180
35	6	-4.034073	-0.387196	-1.028505
36	6	-3.134770	1.012210	-2.764474
37	1	-1.015855	1.390210	-2.597890
38	6	2.356259	-3.300681	-1.018040
39	6	0.696673	-3.225963	-2.756223
40	1	-0.691506	-1.580579	-2.594266
41	6	2.490137	3.457910	-2.177182
42	6	1.548683	4.949338	-0.374391
43	6	3.943394	-1.307570	2.404823
44	6	4.050641	-3.182682	0.722791
45	1	3.566588	0.351537	3.713374
46	6	-3.112219	-2.754566	2.399356
47	6	-4.784947	-1.910233	0.712555
48	1	-1.490841	-3.258955	3.711989
49	1	3.046036	1.992389	-3.640530
50	6	-4.237444	0.418723	-2.179717
51	6	-5.055770	-1.144641	-0.378216
52	1	-3.249204	1.637700	-3.640829
53	6	1.761318	-3.882779	-2.168571
54	6	3.523625	-3.803700	-0.366216
55	1	0.212814	-3.639896	-3.631867
56	1	0.663009	6.068285	1.191478
57	1	2.086643	5.802884	-0.770117
58	1	3.997849	-4.694301	-0.761758
59	1	4.933431	-3.590202	1.200553
60	1	-6.063364	-1.108953	-0.775793
61	1	-5.580997	-2.469283	1.189418
62	5	-1.725477	-4.376596	-0.716204
63	9	-0.648314	-3.947745	0.083606
64	9	-2.260074	-3.272030	-1.416796
65	9	-1.275385	-5.338277	-1.631657
66	9	-2.726144	-4.926799	0.105694
67	5	4.655371	0.689065	-0.721086
68	9	5.630752	0.092828	0.098982
69	9	5.265359	1.556084	-1.638278
70	9	3.959557	-0.323428	-1.419263
71	9	3.750653	1.412456	0.080393
72	5	-2.952890	3.662094	-0.696078
73	9	-2.935524	4.795996	0.136594
74	9	-3.124656	2.507204	0.091903
75	9	-4.004087	3.759946	-1.618289
76	9	-1.723943	3.580977	-1.388923
77	6	-5.578126	0.655884	-2.739985
78	6	-5.838064	0.395755	-4.087839
79	6	-6.587418	1.192576	-1.934124
80	1	-5.055371	-0.023223	-4.713654
81	6	-7.097958	0.650507	-4.618052
82	1	-6.374088	1.428320	-0.895976
83	1	-7.296498	0.433914	-5.663411
84	6	-8.100925	1.181672	-3.810987
85	6	-7.841562	1.457971	-2.470352
86	1	-9.083209	1.384224	-4.227386
87	1	-8.616514	1.885844	-1.841541
88	6	5.159652	-1.727061	3.123887

atom	*Z*	*x*	*y*	*z*
89	6	6.380474	-1.856551	2.452908
90	6	5.100342	-1.968402	4.499968
91	1	6.431951	-1.622600	1.395716
92	6	7.521651	-2.230288	3.152992
93	1	4.151992	-1.873736	5.021222
94	1	8.468546	-2.317282	2.628438
95	6	7.454758	-2.485354	4.520853
96	6	6.242350	-2.353351	5.193105
97	1	8.347483	-2.782715	5.063154
98	1	6.184667	-2.551216	6.259259
99	6	-4.087218	-3.595720	3.116399
100	6	-4.806073	-4.590200	2.444472
101	6	-4.274400	-3.418956	4.490774
102	1	-4.622254	-4.755293	1.388962
103	6	-5.704799	-5.388941	3.141915
104	1	-3.720932	-2.643468	5.012654
105	1	-6.250681	-6.167118	2.616771
106	6	-5.900321	-5.198636	4.507978
107	6	-5.183254	-4.212761	5.181195
108	1	-6.607624	-5.820965	5.048241
109	1	-5.331949	-4.060250	6.245995
110	6	2.226817	-5.164052	-2.724824
111	6	2.578398	-5.264295	-4.073366
112	6	2.270479	-6.303179	-1.914455
113	1	2.547138	-4.379706	-4.702914
114	6	2.987548	-6.484466	-4.599747
115	1	1.963174	-6.232829	-0.875457
116	1	3.271627	-6.552002	-5.645612
117	6	3.032572	-7.615329	-3.788231
118	6	2.667381	-7.523774	-2.446920
119	1	3.348160	-8.568673	-4.201570
120	1	2.687090	-8.406170	-1.814450
121	6	-1.076944	5.344324	3.105774
122	6	-1.571627	6.463504	2.427429
123	6	-0.842195	5.420329	4.482057
124	1	-1.798188	6.385502	1.370201
125	6	-1.818383	7.642784	3.120556
126	1	-0.453120	4.553550	5.008714
127	1	-2.213688	8.504178	2.590406
128	6	-1.567530	7.719156	4.488732
129	6	-1.079653	6.605863	5.168320
130	1	-1.756250	8.644135	5.025627
131	1	-0.882485	6.660146	6.234780
132	6	3.367965	4.498708	-2.737572
133	6	3.274593	4.851199	-4.086434
134	6	4.336891	5.105774	-1.932075
135	1	2.520510	4.382617	-4.712188
136	6	4.126614	5.812870	-4.617933
137	1	4.433194	4.806135	-0.892935
138	1	4.039563	6.090856	-5.663995
139	6	5.087832	6.416774	-3.811223
140	6	5.195390	6.057044	-2.469643
141	1	5.755727	7.164537	-4.228460
142	1	5.953076	6.514978	-1.840967

Table S39. Computed coordinates: $[Cr(Ph_2phen)_3](BF_4)_2$, **1** βααα

atom	*Z*	*x*	*y*	*z*
1	24	-0.004016	-0.398889	-0.045137
2	7	-1.063076	0.910975	1.087798
3	6	-0.879691	2.199113	0.717179
4	6	-1.481037	3.282651	1.375937
5	6	-2.333126	2.992945	2.475087
6	6	-2.488219	1.667810	2.837439
7	6	-1.848318	0.658037	2.120923
8	6	-1.179929	4.600643	0.915582
9	1	-3.133937	1.399850	3.666242
10	1	-1.972302	-0.382152	2.394033
11	7	1.631078	-0.266712	1.152185
12	7	-0.772023	-2.019719	0.916661
13	7	0.481138	1.320499	-1.006357
14	7	-1.620107	-0.751996	-1.232723
15	7	1.285526	-1.562001	-1.111702
16	6	-0.015764	2.421580	-0.399804
17	6	2.705362	-0.935402	0.673875
18	6	1.766565	0.418526	2.275163
19	6	-1.972865	-2.405499	0.421630
20	6	-0.274380	-2.668779	1.956282
21	6	1.245911	1.467391	-2.071420
22	6	-2.452809	-1.686066	-0.716944
23	6	-2.001749	-0.094547	-2.311150
24	6	2.505763	-1.666249	-0.539326
25	6	1.049222	-2.214471	-2.237457
26	6	0.270990	3.725289	-0.829531
27	6	3.955080	-0.948078	1.312228
28	6	2.967614	0.464480	2.981017
29	1	0.889087	0.942317	2.632603
30	6	-2.730877	-3.453085	0.974657
31	6	-0.938613	-3.741236	2.551901
32	1	0.683234	-2.324723	2.327447
33	6	1.587663	2.724027	-2.572042
34	1	1.625699	0.562783	-2.524045
35	6	-3.716726	-1.970279	-1.253292
36	6	-3.241018	-0.308521	-2.917799
37	1	-1.313543	0.646108	-2.694787
38	6	3.543819	-2.441546	-1.082583
39	6	2.012747	-3.019161	-2.844883
40	1	0.060167	-2.098352	-2.663181
41	6	1.137747	3.869385	-1.946942
42	6	-0.344379	4.812775	-0.136681
43	6	4.085184	-0.204947	2.516572
44	6	5.002350	-1.721081	0.724620
45	1	3.021807	1.050917	3.891520
46	6	-2.168239	-4.161864	2.072989
47	6	-4.018560	-3.717449	0.415164
48	1	-0.469098	-4.257603	3.381646
49	1	2.260267	2.790968	-3.418059
50	6	-4.133066	-1.214571	-2.384336
51	6	-4.488942	-3.007134	-0.646298
52	1	-3.520456	0.295077	-3.772733
53	6	3.267545	-3.161550	-2.275862
54	6	4.808395	-2.430945	-0.418039
55	1	1.759531	-3.556869	-3.751562
56	1	-1.626185	5.445738	1.426771
57	1	-0.142180	5.824749	-0.468902
58	1	5.628683	-2.995177	-0.845969
59	1	5.970838	-1.739521	1.209778
60	1	-5.466603	-3.236304	-1.054458
61	1	-4.631320	-4.494734	0.856335
62	5	4.348173	1.772496	-0.794071
63	9	5.536026	1.453680	-0.100572
64	9	4.579223	2.888200	-1.617587
65	9	3.973157	0.670518	-1.588166
66	9	3.332103	2.064015	0.129095
67	5	-4.057522	2.134966	-0.787124
68	9	-4.465676	3.190382	0.056358
69	9	-3.870918	0.970952	-0.022895
70	9	-5.048351	1.907789	-1.759073
71	9	-2.850396	2.492715	-1.418797
72	6	-5.477311	-1.358780	-2.970781
73	6	-5.628878	-1.636463	-4.331557
74	6	-6.615235	-1.171752	-2.178921
75	1	-4.747070	-1.783572	-4.948759
76	6	-6.898794	-1.742826	-4.889378
77	1	-6.498668	-0.919588	-1.129660
78	1	-7.006115	-1.968956	-5.946194
79	6	-8.027649	-1.561241	-4.094815
80	6	-7.882730	-1.270333	-2.739796
81	1	-9.019033	-1.641598	-4.530980
82	1	-8.759972	-1.112910	-2.119195
83	6	5.342319	-0.148953	3.288341
84	6	6.532605	0.297880	2.703942
85	6	5.337956	-0.515357	4.638365
86	1	6.524957	0.621313	1.669270
87	6	7.697738	0.365994	3.460204
88	1	4.416621	-0.866974	5.094278

atom	*Z*	*x*	*y*	*z*
89	1	8.614815	0.724054	3.001201
90	6	7.690643	-0.013924	4.800276
91	6	6.507351	-0.453717	5.388311
92	1	8.603815	0.036760	5.386161
93	1	6.494339	-0.751413	6.432748
94	6	-2.841459	-5.314841	2.698453
95	6	-3.253681	-6.408612	1.928555
96	6	-3.035584	-5.344076	4.083315
97	1	-3.078971	-6.408013	0.856900
98	6	-3.851947	-7.507369	2.534260
99	1	-2.726140	-4.494502	4.685307
100	1	-4.157753	-8.354921	1.928154
101	6	-4.053343	-7.523551	3.912366
102	6	-3.644028	-6.439600	4.685088
103	1	-4.525865	-8.380390	4.383341
104	1	-3.800453	-6.445558	5.759660
105	6	4.261660	-4.044469	-2.915524
106	6	4.578912	-3.870633	-4.266433
107	6	4.865055	-5.084939	-2.200992
108	1	4.118122	-3.060094	-4.823642
109	6	5.495266	-4.712099	-4.887148
110	1	4.602459	-5.245716	-1.159533
111	1	5.743076	-4.560109	-5.933449
112	6	6.093985	-5.744129	-4.168982
113	6	5.772651	-5.931766	-2.826777
114	1	6.807489	-6.403058	-4.654813
115	1	6.227134	-6.742519	-2.265228
116	6	-3.027050	4.049896	3.235785
117	6	-3.877781	4.956103	2.593100
118	6	-2.858764	4.132528	4.621329
119	1	-4.040871	4.861041	1.525535
120	6	-4.540325	5.932353	3.328681
121	1	-2.194806	3.433320	5.121985
122	1	-5.206733	6.625523	2.823443
123	6	-4.358716	6.018331	4.707353
124	6	-3.517608	5.115332	5.352438
125	1	-4.874523	6.785113	5.278078
126	1	-3.371652	5.177048	6.426931
127	6	1.583029	5.189922	-2.429285
128	6	1.398794	5.553666	-3.765781
129	6	2.239762	6.071302	-1.564112
130	1	0.886984	4.872286	-4.439413
131	6	1.849771	6.786159	-4.226298
132	1	2.412668	5.778276	-0.532794
133	1	1.692401	7.064031	-5.264338
134	6	2.499523	7.660848	-3.359168
135	6	2.698296	7.298491	-2.028750
136	1	2.854000	8.621890	-3.720099
137	1	3.216429	7.971246	-1.351741

References

[1] Lin, S.; Ischay, M. A.; Fry, C. G.; Yoon, T. P. *J. Am. Chem. Soc*. **2011**, *133*, 19350-19353.
[2] Stevenson, S. M.; Shores, M. P.; Ferreira, E. M. *Angew. Chem. Int. Ed*. **2015**, *54*, 6506-6510.
[3]Montaliti, M.; Credi, A.; Prodi, L.; Teresa Gandolfi, M. Chemical Actinometry. In *Handbook of Photochemistry,* 3rd ed.; CRC Press: Boca Raton, Fl, 2006; pp 601-616.
[4] Cismesia, M. A.; Yoon, T. P. *Chem. Sci.* **2015,** *6*, 5426.
[5] Crutchley, R. J.; Lever, A. B. P. *Inorg. Chem.* **1982**, *21*, 2276.
[6] Gonzales-Velasco, J.; Rubinstein, I.; Crutchley, R. J.; Lever, A. B. P.; Bard, A. J. *Inorg. Chem.* **1983**, *22*, 822.
[7]Romero, N.; Nicewicz, D. A. *J. Am. Chem. Soc.* **2014**, *136*, 17024-17035
[8]McDaniel, A. M.; Tseng, H. W.; Hill, E. A.; Damrauer, N. H.; Rappé, A. K.; Shores, M. P. *Inorg. Chem.* **2013**, *52*, 1368-1378.